ISSN 1007-9327 (print)
ISSN 2219-2840 (online)

World Journal of *Gastroenterology*

World J Gastroenterol 2024 December 21; 30(47): 4983-5103

Published by Baishideng Publishing Group Inc

World Journal of Gastroenterology

Contents

Weekly Volume 30 Number 47 December 21, 2024

EDITORIAL

ORIGINAL ARTICLE

Retrospective Study

Observational Study

Basic Study

LETTER TO THE EDITOR

ABOUT COVER

AIMS AND SCOPE

The primary aim of *World Journal of Gastroenterology* (*WJG*, *World J Gastroenterol*) is to provide scholars and readers from various fields of gastroenterology and hepatology with a platform to publish high-quality basic and clinical research articles and communicate their research findings online. *WJG* mainly publishes articles reporting research results and findings obtained in the field of gastroenterology and hepatology and covering a wide range of topics including gastroenterology, hepatology, gastrointestinal endoscopy, gastrointestinal surgery, gastrointestinal oncology, and pediatric gastroenterology.

INDEXING/ABSTRACTING

The *WJG* is now abstracted and indexed in Science Citation Index Expanded (SCIE), MEDLINE, PubMed, PubMed Central, Scopus, Reference Citation Analysis, China Science and Technology Journal Database, and Superstar Journals Database. The 2024 edition of Journal Citation Reports® cites the 2023 journal impact factor (JIF) for *WJG* as 4.3; Quartile: Q1. The *WJG*'s CiteScore for 2023 is 7.8.

RESPONSIBLE EDITORS FOR THIS ISSUE

NAME OF JOURNAL
World Journal of Gastroenterology

ISSN
ISSN 1007-9327 (print) ISSN 2219-2840 (online)

LAUNCH DATE
October 1, 1995

FREQUENCY
Weekly

EDITORS-IN-CHIEF
Andrzej S Tarnawski

EXECUTIVE ASSOCIATE EDITORS-IN-CHIEF
Jian-Gao Fan (Chronic Liver Disease)

EDITORIAL BOARD MEMBERS
http://www.wjgnet.com/1007-9327/editorialboard.htm

PUBLICATION DATE
December 21, 2024

PUBLISHING PARTNER
Shanghai Pancreatic Cancer Institute and Pancreatic Cancer Institute, Fudan University
Biliary Tract Disease Institute, Fudan University

INSTRUCTIONS TO AUTHORS
https://www.wjgnet.com/bpg/gerinfo/204

GUIDELINES FOR ETHICS DOCUMENTS
https://www.wjgnet.com/bpg/GerInfo/287

GUIDELINES FOR NON-NATIVE SPEAKERS OF ENGLISH
https://www.wjgnet.com/bpg/gerinfo/240

PUBLICATION ETHICS
https://www.wjgnet.com/bpg/GerInfo/288

PUBLICATION MISCONDUCT
https://www.wjgnet.com/bpg/gerinfo/208

POLICY OF CO-AUTHORS
https://www.wjgnet.com/bpg/GerInfo/310

ARTICLE PROCESSING CHARGE
https://www.wjgnet.com/bpg/gerinfo/242

STEPS FOR SUBMITTING MANUSCRIPTS
https://www.wjgnet.com/bpg/GerInfo/239

ONLINE SUBMISSION
https://www.f6publishing.com

PUBLISHING PARTNER's OFFICIAL WEBSITE
https://www.shca.org.cn
https://www.zs-hospital.sh.cn

World Journal of Gastroenterology

Submit a Manuscript: https://www.f6publishing.com

World J Gastroenterol 2024 December 21; 30(47): 5032-5054

DOI: 10.3748/wjg.v30.i47.5032

ISSN 1007-9327 (print) ISSN 2219-2840 (online)

ORIGINAL ARTICLE

Basic Study

Macrophage-derived cathepsin L promotes epithelial-mesenchymal transition and M2 polarization in gastric cancer

Lu-Xi Xiao, Xun-Jun Li, Hai-Yi Yu, Ren-Jie Qiu, Zhong-Ya Zhai, Wen-Fu Ding, Man-Sheng Zhu, Wu Zhong, Chuan-Fa Fang, Jia Yang, Tao Chen, Jiang Yu

Specialty type: Gastroenterology and hepatology

Provenance and peer review: Unsolicited article; Externally peer reviewed.

Peer-review model: Single-blind

Peer-review report's classification

Scientific Quality: Grade B, Grade B, Grade C, Grade C

Novelty: Grade B, Grade B, Grade B, Grade C

Creativity or Innovation: Grade B, Grade B, Grade B, Grade B

Scientific Significance: Grade B, Grade B, Grade B, Grade B

P-Reviewer: Aktas G; Wang XB; Yari D

Received: June 17, 2024

Revised: September 11, 2024

Accepted: October 13, 2024

Published online: December 21, 2024

Processing time: 161 Days and 21.3 Hours

Lu-Xi Xiao, Xun-Jun Li, Hai-Yi Yu, Ren-Jie Qiu, Zhong-Ya Zhai, Wen-Fu Ding, Man-Sheng Zhu, Tao Chen, Jiang Yu, Department of General Surgery, Guangdong Provincial Key Laboratory of Precision Medicine for Gastrointestinal Tumor, Nanfang Hospital, Southern Medical University, Guangzhou 510515, Guangdong Province, China

Wu Zhong, Chuan-Fa Fang, Tao Chen, Department of Gastrointestinal and Hernia Surgery, Ganzhou Hospital-Nanfang Hospital, Ganzhou 341099, Jiangxi Province, China

Jia Yang, Department of Gastrointestinal Surgery, Central Hospital of Wuhan, Wuhan 430014, Hubei Province, China

Jia Yang, Department of General Surgery, Xiangyang Central Hospital, The Affiliated Hospital of Hubei University of Arts and Science, Xiangyang 441021, Hubei Province, China

Co-first authors: Lu-Xi Xiao and Xun-Jun Li.

Co-corresponding authors: Tao Chen and Jiang Yu.

Corresponding author: Jiang Yu, MD, Adjunct Professor, Doctor, Department of General Surgery, Guangdong Provincial Key Laboratory of Precision Medicine for Gastrointestinal Tumor, Nanfang Hospital, Southern Medical University, No. 1023 Shatai South Road, Baiyun District, Guangzhou 510515, Guangdong Province, China. balbc@163.com

Abstract

BACKGROUND

Advanced gastric tumors are extremely prone to metastasize the in 20%–30% of gastric cancer, and patients have a poor prognosis despite systemic chemotherapy. Peritoneal metastases from gastric cancer usually indicate the end stage of the disease without curative treatment.

AIM

To peritoneal metastasis for facilitating clinical therapy are urgently needed.

METHODS

Immunohistochemical staining and immunofluorescence staining were used to demonstrate the high expression of cathepsin L (CTSL) in human gastric cancer tissues and its localization in cells. Lentivirus transfection was used to construct

stable cell lines. Transwell invasion assays, wound healing assays, and animal tests were used to determine the relationships between CTSL and epithelial-mesenchymal transition (EMT) and tumorigenic potential *in vivo*.

RESULTS

We observed that macrophage-derived CTSL promoted gastric cancer cell migration and metastasis *via* the EMT pathway *in vitro* and *in vivo*, which involved macrophage polarization. Our findings suggest that macrophages improve extracellular matrix remodeling and hence facilitate tumor metastasis. Ablation of CTSL in macrophages within the tumor microenvironment may improve tumor therapy and the prognosis of patients with gastric cancer peritoneal metastasis.

CONCLUSION

In consideration of our findings, tumor-associated macrophage-derived CTSL is an important factor that promotes the metastasis and invasion of gastric cancer cells, and the targeting of CTSL may potentially improve the prognosis of patients with gastric cancer with peritoneal metastasis.

Key Words: Gastric cancer; Invasion and metastasis; Epithelial-mesenchymal transition; Inflammation; Immunology; Tumor-associated macrophages; Cancer prevention

Core Tip: Advanced gastric tumors are extremely prone to metastasize into the peritoneum and herald a dismal prognosis with limited therapeutic options. Certain intraperitoneal chemotherapies have been examined, but their response is still underperforming. Discovering target molecules associated with the development of gastric cancer peritoneal metastasis (GCPM) is critical for improving clinical therapy. In our study, we revealed that tumor-associated macrophage-derived cathepsin L can significantly facilitate gastric cancer invasion and metastasis both *in vitro* and *in vivo*. Immune-related therapy may be a promising approach to improve the prognosis of patients with GCPM.

Citation: Xiao LX, Li XJ, Yu HY, Qiu RJ, Zhai ZY, Ding WF, Zhu MS, Zhong W, Fang CF, Yang J, Chen T, Yu J. Macrophage-derived cathepsin L promotes epithelial-mesenchymal transition and M2 polarization in gastric cancer. *World J Gastroenterol* 2024; 30(47): 5032-5054

URL: https://www.wjgnet.com/1007-9327/full/v30/i47/5032.htm

DOI: https://dx.doi.org/10.3748/wjg.v30.i47.5032

INTRODUCTION

Peritoneal carcinomatosis (PC) is known as an orphan disease with a dismal prognosis and limited therapeutic options; PC comprises primary peritoneal mesothelioma and secondary peritoneal metastases (PMs) of other tumors. Notably, the incidence of secondary PC greatly exceeds that of primary PC, with the highest prevalence in patients with gastric and ovarian cancer[1]. Five population-based studies from the United States and the Netherlands reported that the incidence of peritoneal metastasis (PM) from gastric cancer ranged from 14% to 41%, and 58% of diffuse-type carcinomas metastasized to the peritoneum rather than other sites (liver, lungs, and bones)[2]. However, the detailed mechanisms of PC deserve further exploration.

The epithelial-mesenchymal transition (EMT) is recognized as a classical pathway for tumor metastasis that converts epithelial cells into mesenchymal cells with decreased adhesive ability[3]. Inhibiting the degradation of adhesion molecules in the extracellular matrix (ECM) may be an effective approach for alleviating EMT and potential peritoneal metastasis. A typical modulator in the ECM, cathepsin L (CTSL), is upregulated in various malignancies, including breast, lung, gastric, colon, head and neck carcinomas, melanomas, and gliomas[4]. As a chief member of the lysosomal cysteine protease family, CTSL is considered to play an important physiological role in the catabolism of proteins in the lysosomal system and is considered a potential therapeutic target in cancer treatment. In gastric cancer, CTSL exists in a high-molecular-weight form. A structural change in the sugar chains of a glycoprotein produced by cells has been proposed to be associated with the malignant transformation of CTSL, which also contributes to its more stable enzymatic structure. The activity of CTSL in gastric cancer tissue and its alkaline and heat stability properties suggest that CTSL contributes to gastric cancer invasion[5]. Over the past few decades, CTSL reduction or ablation has been considered to abolish apoptosis and angiogenesis in tumors[6,7], resulting in decreased invasiveness and metastasis[8,9]. In particular, CTSL is upregulated in gastric tumors with muscularis propria and venous invasion, as well as in chronic atrophic gastritis with intestinal metaplasia, suggesting its role in the transition of gastritis to malignancy[10,11]. In 2020, Pan *et al*[12] revealed that CTSL can promote angiogenesis by regulating the CCAAT-displacement protein/cut homeobox/vascular endothelial growth factor-D pathway in human gastric cancer. However, the exact mechanism of CTSL in gastric cancer metastases has rarely been reported and requires further investigations.

Peritoneal metastasis is associated with inflammation[13]. In addition, inflammation and inflammatory cells are involved in various types of cancers, including colon[14] and gastric[15] cancers. Furthermore, CTSL has regulatory effects on inflammation[16]. Macrophages are recruited to lesions and can be utilized by tumor cells to exert protumor effects[17]. Cathepsins, such as cathepsin B (CTSB), CTSL, and cathepsin S (CTSS), have been reported to be expressed in macrophages[18]. In addition, human monocyte-derived macrophages have been found to synthesize both elastolytic matrix metalloproteinases (MMPs) and cysteine proteinases, but only fully processed cathepsins have been detected in the ECM. Coculture of a colon tumor cell line and monocytes significantly increased CTSB expression in both tumor cells and normal cells within the tumor microenvironment, increasing the invasive ability of tumor cells five-fold[19]. These studies highlight the protumor function of macrophage-derived cathepsins in cancers. Here, we observed increased CTSL in gastric cancer and aimed to identify its role and association with macrophages in the gastric tumor environment, which has rarely been reported until now.

MATERIALS AND METHODS

Patients and tissue samples

Primary gastric cancer tissue samples and peritoneal node samples were obtained from 53 patients who underwent curative resection at Nanfang Hospital of Southern Medical University between 2015 and 2021. In addition, 38 gastric cancer surgical resection samples from The Central Hospital of Wuhan collected between 2020 and 2021 were included in our study. The collected samples consisted of tumor tissue (T, avoiding the selection of necrotic areas within the tumor), adjacent normal tissue (N, located > 5 cm away from the tumor edge), and peritoneal metastatic nodes (M, confirmed by pathological identification). All patients had not received any prior treatment, such as chemotherapy, radiotherapy, or biological therapy, before surgery.

All collected samples were pathologically diagnosed as gastric cancer, and all related procedures were performed with the approval of The Ethics Committee of Nanfang Hospital and the Central Hospital of Wuhan, No. NFEC-2021-008. Formalin-fixed, paraffin-embedded cancer specimens were obtained from patients with informed consent. Patient information, including patient name, age, surgical date, pathological number, pathological data, and preoperative diagnosis and treatment history, was collected. Patients enrolled in this study met the following inclusion criteria: (1) Clear pathological diagnosis of gastric adenocarcinoma without other tumors; (2) No preoperative antitumor therapy; and (3) No other distant organ metastases except for peritoneal metastasis.

Cell culture and reagents

The human gastric cancer cell lines (MKN45 and MGC803) and the human monocytic cell line THP-1 were preserved in a liquid nitrogen jar at The General Surgery Laboratory of Nanfang Hospital (purchased from Shanghai Cell Bioscience Inc.). The cells were cultured in RPMI 1640 medium (Gibco, United States) supplemented with 10% fetal bovine serum (FBS) (Gibco, United States) at 37 °C in a humidified atmosphere with 5% CO_2. For macrophage generation, THP-1 cells (1×10^6 cells) were treated with 100 ng/mL phorbol ester (Sigma-Aldrich, United States) for 24 hours. Gastric cancer cell line and macrophage cocultivation was conducted *via* a noncontact transwell system in 6-well plates (Corning, United States). Inserts containing THP-1-derived macrophages were transferred into a 6-well plate previously seeded with gastric cancer cells (1×10^5 cells). After 48 hours of coculture, the gastric cancer cells or macrophages were harvested for further analysis.

Generation of stable cell lines via lentiviral transfection

The recombinant human CTSL-shRNA-LV lentiviral vector and its control Scr-shRNA-LV viral vector were produced by the Genechem Company (Shanghai, China) according to the following target RNA interference sequences: CTSL siRNA-1 sense strand: 5'-GCCUCAGCUACUCUAACAU-3', CTSL siRNA-2 sense strand: 5'-CCAAGUAUUCUGUUGCUAATT-3.

THP-1 cells (1×10^5 cells/mL) were infected by incubation with a concentrated lentiviral vector overnight in the presence of 6 mg/mL polybrene. After 48 hours to 72 hours, the cells were observed *via* a microscope. The cells were further cultured in RPMI 1640 containing 10% FBS supplemented with 5 mg/mL puromycin under humidity and 10% CO_2 at 37 °C for selection and growth. Simultaneously, the cells were collected for quantitative real-time polymerase chain reaction (qRT-PCR) and western blotting to examine the expression levels of the target genes.

Transwell invasion assay

The invasion assay was performed using 24-well transwells (6.5 mm diameter, 8.0 mm pore size; Corning, United States) precoated with Matrigel (Corning, United States) and incubated at 37 °C for three hours for solidification. A total of 5×10^4 cells (MKN45 or MGC803 cells) suspended in 200 mL of RPMI 1640 were added to the top of the Matrigel in the upper chamber and cultured with THP-1 cells or THP-1 $CTSL^{KD}$ cells seeded with 700 mL of RPMI 1640 containing 10% FBS in the lower chamber. After 48 hours of coculture, the Matrigel and remaining cells in the upper chamber were removed with cotton swabs. The cells on the lower surface of the membrane were fixed in 4% paraformaldehyde and stained with 0.5% crystal violet. The stained cells in 5 random microscopic fields (at 400 × magnification) were counted and captured. All the experiments were performed in triplicate.

Wound healing assay

The ability of gastric cancer cells to migrate following culture with macrophages was evaluated *via* a wound healing

assay. MKN45 or MGC803 cells (1 × 10^5 cells) were seeded and grown to 80%–90% confluence in 6-well plates, and a scratch was made by dragging a 200 μL pipette tip across the cell surface. The remaining cells were washed with phosphate-buffered saline (PBS) to avoid cellular debris and cocultured with noncontact transwell inserts (24 mm diameter, 0.4 mm pore size; Corning, United States) containing THP-1 cells or THP-1 $CTSL^{KD}$ cells. The migrating tumor cells at the wound front were photographed at 6 hours, 12 hours, 24 hours, 36 hours, and 48 hours. All the experiments were performed in triplicate. The area of the wound was calculated *via* Image J software (National Institutes of Health, United States).

RNA extraction and qRT-PCR

Total RNA was extracted from cells or tissues *via* TRIzol™ Reagent (Gibco, United States) according to the manufacturer's protocol. After detection of the RNA concentration, 500 ng of total RNA was reverse transcribed to cDNA *via* HiScript® II Q RT SuperMix for qPCR (Vazyme, China). The cDNA and forward and reverse primers were used for subsequent qRT-PCR with SYBR-Green PCR Master Mix (No. 11202ES08; YEASEN). Reverse transcription and qRT-PCR were performed *via* the Biometra TRIO amplification instrument and Applied Biosystems QuantStudio 5 (Thermo Fisher Scientific, United States). Relative gene expression data were analyzed *via* the $2^{-\Delta\Delta Ct}$ method. In cell or tissue lysates, the mRNA levels were normalized to those of β-actin. The mean value of β-actin in the control group was set as the reference value. The sequences of the primers used in the study are shown in Supplementary Table 1.

Western blot

A total of 40 mg of protein extracted from cells with RIPA lysis buffer (No. FD008; Fdbio Science, China) was separated on a 10% sodium dodecyl sulfate polyacrylamide gel under constant voltage. Proteins were blotted onto a 0.22 mm polyvinylidene fluoride membrane (No. ISEQ00010; Merck Millipore, Germany) under constant current. The membranes were blocked in 5% skim milk at room temperature for one hour and incubated with primary antibody at 4 °C overnight. Next, the membranes were incubated with horseradish peroxidase (HRP)-conjugated secondary antibodies for one hour at room temperature. For each incubation, the membranes were washed three times for 5 minutes each with tris-buffered saline-Tween 20. Finally, the blots were detected with an enhanced chemiluminescence solution using a chemiluminescence detection system (No. 5200; Tanon, China). The following primary antibodies were purchased: (1) anti-CTSL (1:1000; Proteintech, United States); (2) Anti-E-cadherin (1:1000; Cell Signaling, United States); (3) Anti-N-cadherin (1:1000; Cell Signaling, United States); (4) Anti-Snail (1:1000; Cell Signaling, United States); (5) Anti-β-catenin (1:1000; Cell Signaling, United States); and (6) Anti-β-actin (1:2000; Proteintech, United States).

Immunohistochemistry

Immunohistochemistry (IHC) staining of human gastric cancer specimens and murine subcutaneous tumors was performed according to the following protocol. Consecutive paraffin sections (4 mm) were cut and mounted on adhesive slides coated with 3-aminopropyl-trienthoxysilane. The sections were heated at 65 °C for two hours and then deparaffinized in xylene and a graded series of ethanol solutions (from 100% to 75% concentrations). Antigen retrieval was performed in a high-pressure cooker for 5 minutes in 0.01 M sodium citrate buffer [pouvoir hydrogène (pH) of 6.0] (BOSTER, China), after which the samples were incubated with 3% hydrogen peroxide for 10 minutes to quench endogenous peroxidase activity. The sections were incubated with 5% goat serum for one hour at room temperature, followed by incubation with primary antibodies at 4 °C overnight. After incubation with HRP-conjugated anti-mouse or HRP-conjugated anti-rabbit antibodies for one hour at room temperature, immunostaining was performed using 3,3′-diaminobenzidine tetrahydrochloride (DAB; Zsbio Bioscience, China) according to the manufacturer's instructions. For the negative control, isotype-matched antibodies were applied. Subsequently, the nuclei were counterstained with Mayer's hematoxylin (Solarbio, China). The sections were dehydrated in an ascending series of ethanol solutions (from 75% to 100% concentrations) and xylene. Finally, coverslips were placed on the slides with neutral balsam (Solarbio, China). The following primary antibodies were purchased: (1) Anti-CTSL (1:400; Proteintech, United States); (2) Anti-CD68 (1:500; Abcam, United States); (3) Anti-E-cadherin (1:400; Cell Signaling, United States); and (4) Anti-Ki67 (1:500; Abcam, United States). Multiple IHC (mIHC) was performed *via* an mIHC kit (abs50012, Absin; China) according to the manufacturer's instructions.

The number of cells stained with antibodies was calculated per field of view *via* a microscope, with 5 fields of view per section evaluated at 400 × magnification. The expression levels of CTSL, E-cadherin, and CD68 were analyzed with Image J (NIH, United States). The percentage of positive cells was calculated.

Immunofluorescence

For cell staining, before fixation, nonadherent and semiadherent cells in confocal dishes were removed by washing with PBS, and the adherent cells were analyzed *via* an immunofluorescence (IF) assay. The cells were fixed with 4% PFA at room temperature for 30 minutes and then incubated with 5% goat serum for one hour at room temperature. For tissue staining, IF was performed in the same manner as for the IHC staining procedures before the antibody incubation. After nonspecific antigens were blocked, the dishes or tissue sections were incubated with a combination of primary antibodies, including anti-CTSL (1:400; Proteintech, United States), anti-CD68 (1:500; Abcam, United States), anti-CD163 (1:200; Abcam, United States), or anti-CD86 (1:200; Abcam, United States) at 4 °C overnight, followed by incubation with fluorescein-conjugated secondary antibodies, such as goat anti-rabbit immunoglobulin G (IgG) H and L (Alexa Fluor® 488) (1:500; Abcam, United States), goat anti-rabbit IgG H and L (Alexa Fluor® 594) (1:500; Abcam, United States), and goat anti-mouse IgG H and L (Alexa Fluor® 647) (1:500; Abcam, United States). Nuclear staining was performed with 4',6-diamidino-2-phenylindole (Solarbio, China). IF images were captured *via* a Zeiss LSM 5 confocal microscope and

analyzed with Zen software (Zeiss, Germany) and Image J.

Animal studies

To verify the protumoral effects of macrophage-derived CTSL, we established a murine model with subcutaneous tumors *in vivo*. All the animals were fed and monitored at The Animal Experiment Center of Nanfang Hospital with specific pathogen-free microorganism grade. In addition, all of their feeding and experiments were performed in The Southern Medical University animal facility with 12-hour day or night cycles according to the guidelines for the use of laboratory animals. The research experiments in our study did not involve more than momentary pain or distress and did not require the use of pain-relieving drugs. The animal experiments were approved by The Animal Ethics Committee of Nanfang Hospital (No. IACUC-LAC-20230717-008). Six-week-old male BALB/c nude mice (purchased from Zhuhai Bestest Bioscience Ltd) were divided into four randomized groups (n = 5 per group), and the same group of animals was housed in the same cage. MKN45 cells alone (5 × 10^5 cells), shNC tumor-associated macrophages (TAMs) alone (5 × 10^5 cells), MKN45 cells (5 × 10^5 cells) and shNC TAMs (5 × 10^5 cells), or MKN45 cells (5 × 10^5 cells) and shCTSL TAMs (5 × 10^5 cells) in 100 μL were subcutaneously injected into the flank of each mouse. The design, execution and analysis of the experiment were performed independently by different people to conceal the grouping of the experimental animals. After 3 days, we measured the tumor size [anteroposterior diameter (L), transverse diameter (W), and height (H)] every 3 days *via* a digital vernier caliper and calculated the tumor volume according to the following formula: V = p/6 × L × W × H (mm^3). Three weeks after cell injection, the mice were sacrificed, and the tumors were collected and visually examined. There are no inclusion or exclusion criteria for experimental animals, and data from all experimental units and time points are included. The original data include handwritten records from our laboratory. The tumor tissues of the mice were further examined *via* haematoxylin and eosin (HE) and IHC staining.

Statistical analysis

All the statistical analyses were performed *via* Statistical Package for the Social Sciences statistical software (version 25.0, IBM SPSS, United States) and GraphPad Prism (version 9.0, GraphPad Software, United States) for Windows. Pearson's correlation analysis was used to assess the relationships among CD68, CD163, and CTSL expression in patient tissues. The Student's t test was used to analyze the differences between the data from the two groups. One-way analysis of variance (ANOVA) was used for comparisons among three or more groups. Dunnett's multiple comparisons test was performed to compare all the groups with the control group. All the data were examined using normality tests (Shapiro-Wilk test). Several groups with a nonnormal distribution were analyzed by the Wilcoxon signed rank test. All the cell culture experiments were performed in triplicate. All values are presented as the means ± SD. The significance levels are denoted as $^aP < 0.05$, $^bP < 0.01$, $^cP < 0.001$, and nonsignificant when the P value exceeds 0.05.

RESULTS

Human gastric cancer with peritoneal metastasis highly expresses CTSL

The regulation of CTSL activity involves endogenous cathepsin inhibitors (cystatins and stefins)[20] and the activation of their inactive precursors by autolysis in the acidic pH environment of lysosomes[9,21]. In addition, external hypoxic and acidic conditions can also induce CTSL secretion by increasing CTSL expression and lysosomal exocytosis[22]. Therefore, the local tumor environment, which is acidified due to increased anaerobic glycolysis, may improve the activity of extracellular CTSL.

We searched for CTSL in the Gene Expression Profiling Interactive Analysis platform *via* The Cancer Genome Atlas database and detected the upregulation of CTSL in multiple cancers, including *SKCM*, *DLBC*, *GBM*, *THYM*, and *STAD* (Figure 1A). CTSL was more highly expressed in gastric tumors (n = 408) than in normal tissues (n = 211) in patients with STAD ($^aP < 0.05$) (Figure 1B), and its expression was associated with tumor stage (P = 0.00892) (Figure 1C). Moreover, GEO2R analysis revealed differentially expressed genes in two Gene Expression Omnibus datasets of gastric cancer, GSE33651 and GSE118916 (log2fc = 1.786, log2fc = 2.162) (Figure 1D).

Next, we detected the mRNA expression of CTSL in 64 pairs of human gastric cancer tissues and paracancerous normal tissues from patients at Nanfang Hospital *via* qRT-PCR and detected differential expression between the two groups (P = 0.0412) (Figure 1E). Furthermore, we compared CTSL mRNA expression between patients with metastasis (M1, n = 12) and without metastasis (M0, n = 45) and confirmed a positive correlation between CTSL and gastric tumor metastasis (P = 0.0434) (Figure 1F). On the basis of the above results, we explored the underlying mechanism by which CTSL influences gastric tumor metastasis.

To further identify the expression and location of CTSL in gastric cancer tissues, we performed IHC staining on 53 paraffin sections of human gastric cancer and paired paracancerous normal tissues from Nanfang Hospital (with metastasis: 18 cases; without metastasis: 35 cases) and 38 paraffin sections of human gastric cancer from The Central Hospital of Wuhan (with metastasis: 9 cases; without metastasis: 29 cases) (Table 1). Statistical analysis revealed extensively increased expression of CTSL in gastric cancer tissues ($^cP < 0.001$) (Figure 1G and H), and patients with peritoneal metastasis in two centers were more likely to highly express CTSL ($^aP < 0.05$ and $^cP < 0.001$) (Figure 1I-K).

Next, we recognized the tumor margin, defined as a 2-mm-wide region extending from the tumor front to where no tumor cells exist according to previous studies[23,24], in all sections (Figure 2A). We unexpectedly discovered that, within the tumor tissues, CTSL expression in the tumor margin was significantly upregulated compared with that in the tumor bulk ($^cP < 0.001$) (Figure 2B and C), which was more obvious in the group with peritoneal metastasis ($^cP < 0.001$) (Figure 2D) than in the group without peritoneal metastasis ($^bP < 0.01$) (Figure 2E). Only the patients with peritoneal

Table 1 Demographic data of the patients enrolled in our study, *n* (%)

Characteristic	Overall (*n* = 91)	PM (-) (*n* = 64)	PM (+) (*n* = 27)	*P* value[1]
Sex				0.479
Female	20.00 (25.97)	16.00 (28.07)	4.00 (20.00)	
Male	57.00 (74.03)	41.00 (71.93)	16.00 (80.00)	
Unknown	14	7	7	
Patient age, median (interquartile range)	63.00 (56.00–69.00)	64.00 (58.00–71.00)	62.00 (52.00–66.00)	0.121
Unknown	14	7	7	
T stage				0.304
1	5.00 (6.49)	5.00 (8.77)	0.00 (0.00)	
2	5.00 (6.49)	5.00 (8.77)	0.00 (0.00)	
3	13.00 (16.88)	10.00 (17.54)	3.00 (15.00)	
4	54.00 (70.13)	37.00 (64.91)	17.00 (85.00)	
Unknown	14	7	7	
N stage				< 0.001
x	7.00 (9.09)	0.00 (0.00)	7.00 (35.00)	
0	18.00 (23.38)	16.00 (28.07)	2.00 (10.00)	
1	13.00 (16.88)	12.00 (21.05)	1.00 (5.00)	
2	13.00 (16.88)	11.00 (19.30)	2.00 (10.00)	
3	26.00 (33.77)	18.00 (31.58)	8.00 (40.00)	
Unknown	14	7	7	
M stage				< 0.001
0	57.00 (74.03)	57.00 (100.00)	0.00 (0.00)	
1	20.00 (25.97)	0.00 (0.00)	20.00 (100.00)	
Unknown	14	7	7	
Stage				< 0.001
I	6.00 (7.79)	6.00 (10.53)	0.00 (0.00)	
II	17.00 (22.08)	17.00 (29.82)	0.00 (0.00)	
III	34.00 (44.16)	34.00 (59.65)	0.00 (0.00)	
IV	20.00 (25.97)	0.00 (0.00)	20.00 (100.00)	
Unknown	14	7	7	

[1]Pearson's χ^2; Wilcoxon rank sum test; Fisher's exact test.

metastasis had significantly different CTSL expression between the tumor margin and bulk ($^cP < 0.001$) (Figure 2F and G). Similarly, gastric cancer tissues from patients with PM presented increased CTSL levels in the tumor margin but not in the tumor bulk ($^aP < 0.05$ and $^cP < 0.001$) (Figure 2H). Similar results were obtained with the stained gastric cancer sections from the Central Hospital of Wuhan cohort (Supplementary Figure 1).

Macrophage-derived CTSL promotes gastric cancer cell invasion, migration, and EMT progression in coculture

Despite its widespread expression in nearly all normal and neoplastic tissues, the function of most normal tissues depends on intracellular CTSL, but tumor-associated and metastasis-associated properties are mediated primarily *via* extracellular CTSL[25]. When the IHC sections were scanned, we observed positive staining of multinucleated giant cells in the gastric tumor tissues from different patients (Figure 3A). Generally, macrophages within the tumor microenvironment are frequently observed at the break of the basement membrane in the early stage of malignant transformation and at the invasive front of advanced tumors, improving angiogenesis and ECM degradation and remodeling[26].

Therefore, we performed IF staining, which revealed high colocalization of CTSL and CD68 (a marker of mononuclear macrophages) in the tumor tissues of gastric cancer patients (Figure 3B), suggesting that macrophages, the multinucleated giant cells shown in Figure 3A, are the main source of CTSL in gastric cancer. Notably, macrophages at the leading edge

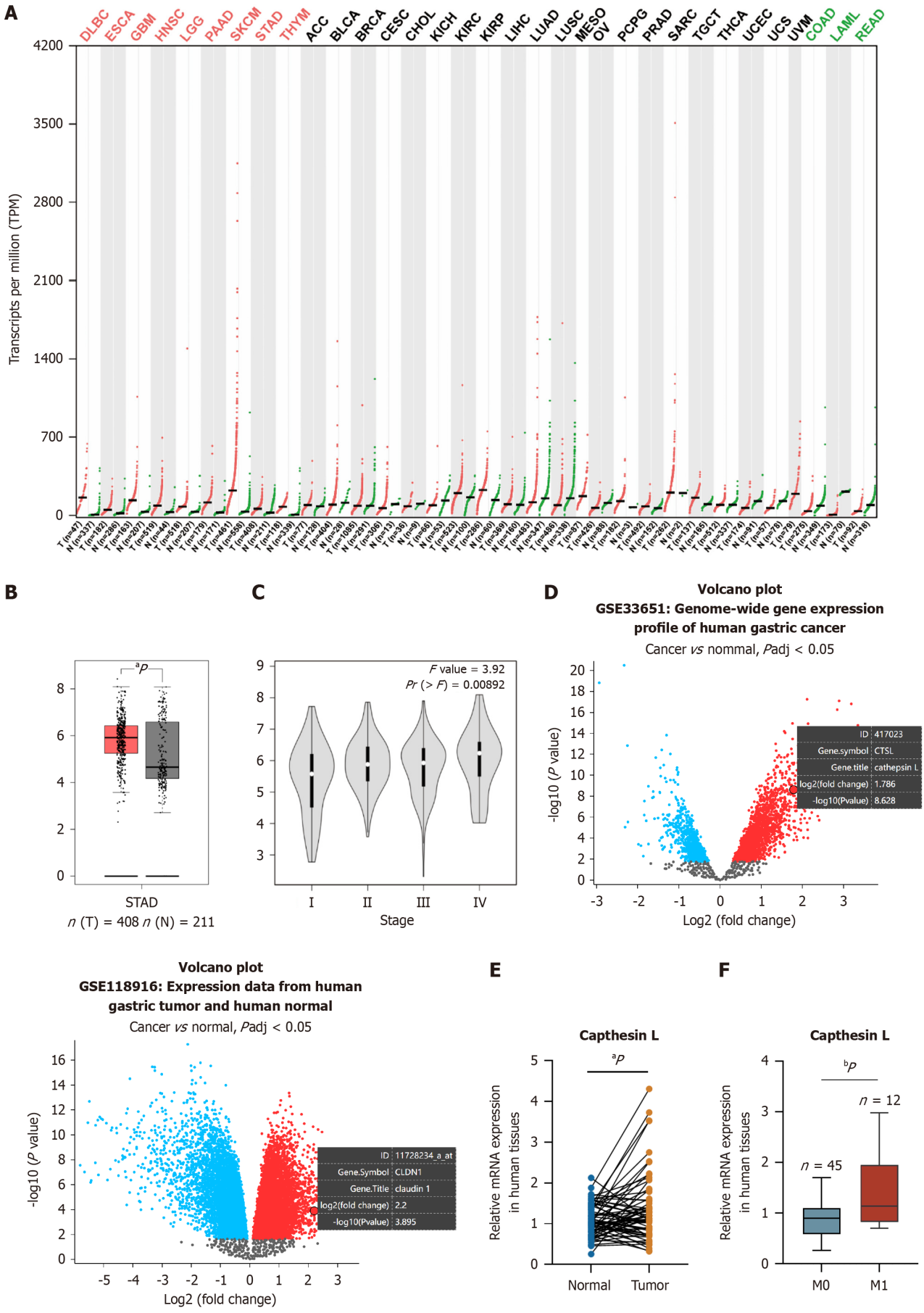
A
DLBC ESCA GBM HNSC LGG PAAD SKCM STAD THYM ACC BLCA BRCA CESC CHOL KICH KIRC KIRP LIHC LUAD LUSC MESO OV PCPG PRAD SARC TGCT THCA UCEC UCS UVM COAD LAML READ
Transcripts per million (TPM)
4200
3500
2800
2100
1400
700
0
B
aP
STAD
n (T) = 408 n (N) = 211
C
F value = 3.92
Pr (> F) = 0.00892
I II III IV
Stage
D
Volcano plot
GSE33651: Genome-wide gene expression profile of human gastric cancer
Cancer vs nommal, Padj < 0.05
-log10 (P value)
Log2 (fold change)
ID 417023
Gene.symbol CTSL
Gene.title cathepsin L
log2(fold change) 1.786
-log10(Pvalue) 8.628
Volcano plot
GSE118916: Expression data from human gastric tumor and human normal
Cancer vs normal, Padj < 0.05
-log10 (P value)
Log2 (fold change)
ID 11728234_a_at
Gene.Symbol CLDN1
Gene.Title claudin 1
log2(fold change) 2.2
-log10(Pvalue) 3.895
E
Capthesin L
aP
Relative mRNA expression in human tissues
Normal Tumor
F
Capthesin L
bP
n = 12
n = 45
Relative mRNA expression in human tissues
M0 M1

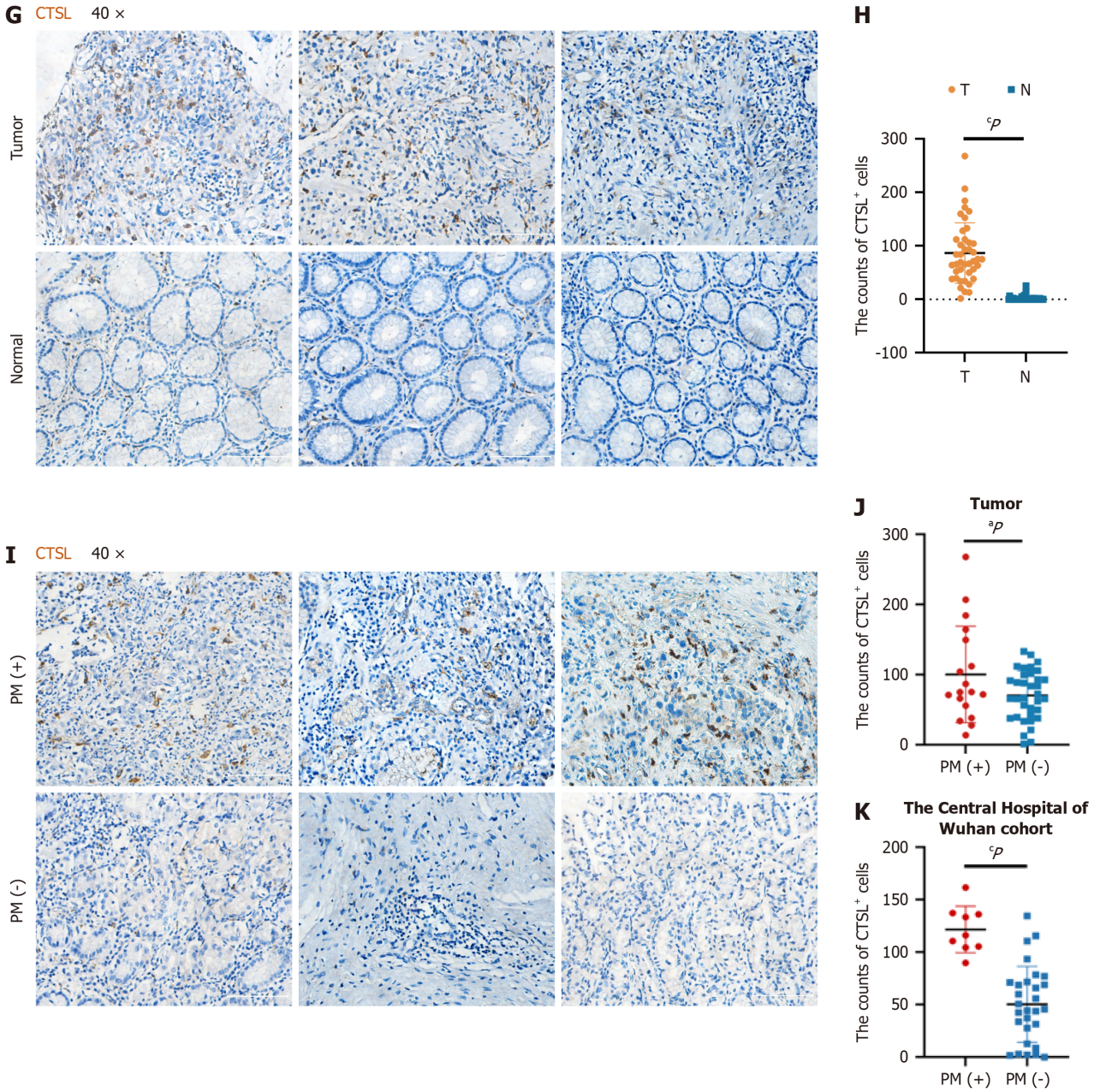

Figure 1 Upregulated expression of cathepsin L in gastric cancer patients with peritoneal metastasis. A: The general level of cathepsin L (CTSL) expression among different cancers from the Gene Expression Profiling Interactive Analysis platform in The Cancer Genome Atlas database; B and C: CTSL expression in gastric tumors (n = 408) was significantly greater than that in normal gastric tissues (n = 211) and was associated with tumor stage in the STAD dataset. The error bars represent the SD, $^{a}P < 0.05$ according to Student's t test; D: As a differentially expressed gene, *CTSL* was upregulated in GSE33651 and GSE11896 (log2fc = 1.786, log2fc = 2.162) *via* GEO2R analysis; E and F: The qPCR analysis of mRNAs extracted from 64 paired gastric tissues from patients at Nanfang Hospital revealed a significant increase in CTSL expression in tumor tissues (n = 64), P = 0.0412, especially in the group with metastasis (n = 12), P = 0.0434. The data points are presented as the means ± SD. The error bars represent the SD. $^{a}P < 0.05$ according to Student's t test; $^{b}P < 0.01$ according to Student's t test; G and H: Representative immunohistochemistry (IHC) images of tumor and paracancerous normal sections stained for CTSL; scale bar, 100 μm. The quantification of positively stained cells in the sections *via* Image J was performed *via* the geometric mean of 3 representative views from each section; the 53 sections from Nanfang Hospital were used in total. The error bars represent the SD; $^{c}P < 0.001$ according to Student's t test; I-K: Representative IHC images of tumor sections from patients with or without peritoneal metastasis stained for CTSL; the error bars represent the SD; $^{a}P < 0.05$; $^{c}P < 0.001$ according to Student's t test. The quantification of positively stained cells in the sections was the same as above for 53 sections from Nanfang Hospital (with metastasis: 18 cases; without metastasis: 35 cases) and 39 sections from the Central Hospital of Wuhan (with metastasis: 9 cases; without metastasis: 30 cases) were used for each group. T: Tumor; N: Normal; PM: Peritoneal metastasis; CTSL: Cathepsin L.

of tumors drive the invasive cellular phenotype partially through a paracrine positive feedback signaling loop, which involves tumor-derived colony growth factor (colony stimulating factor-1) and macrophage-derived epidermal growth factor[26,27]. Our findings suggest that CTSL may be another tumor-associated macrophage (TAM)-secreted molecule involved in promoting tumor dissemination and metastasis.

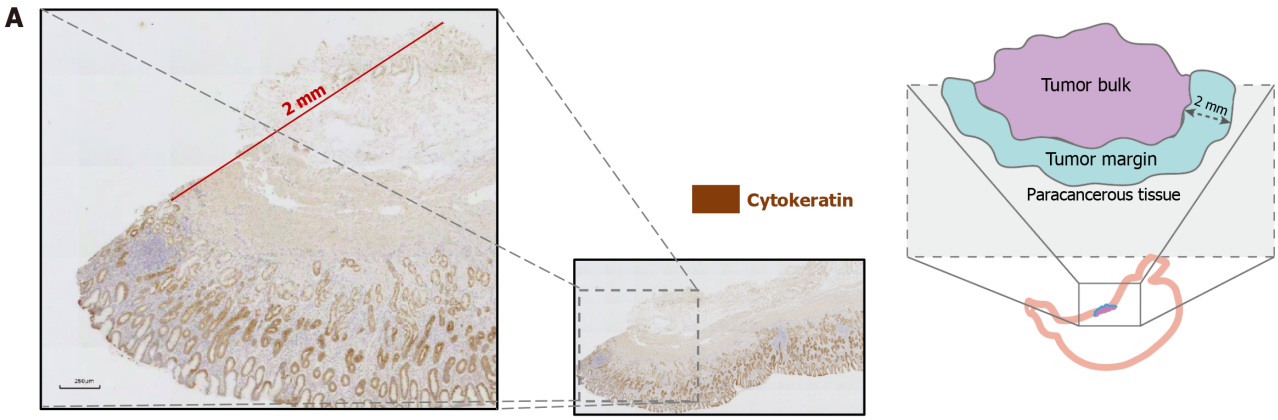
A
2 mm
Cytokeratin
Tumor bulk
2 mm
Tumor margin
Paracancerous tissue

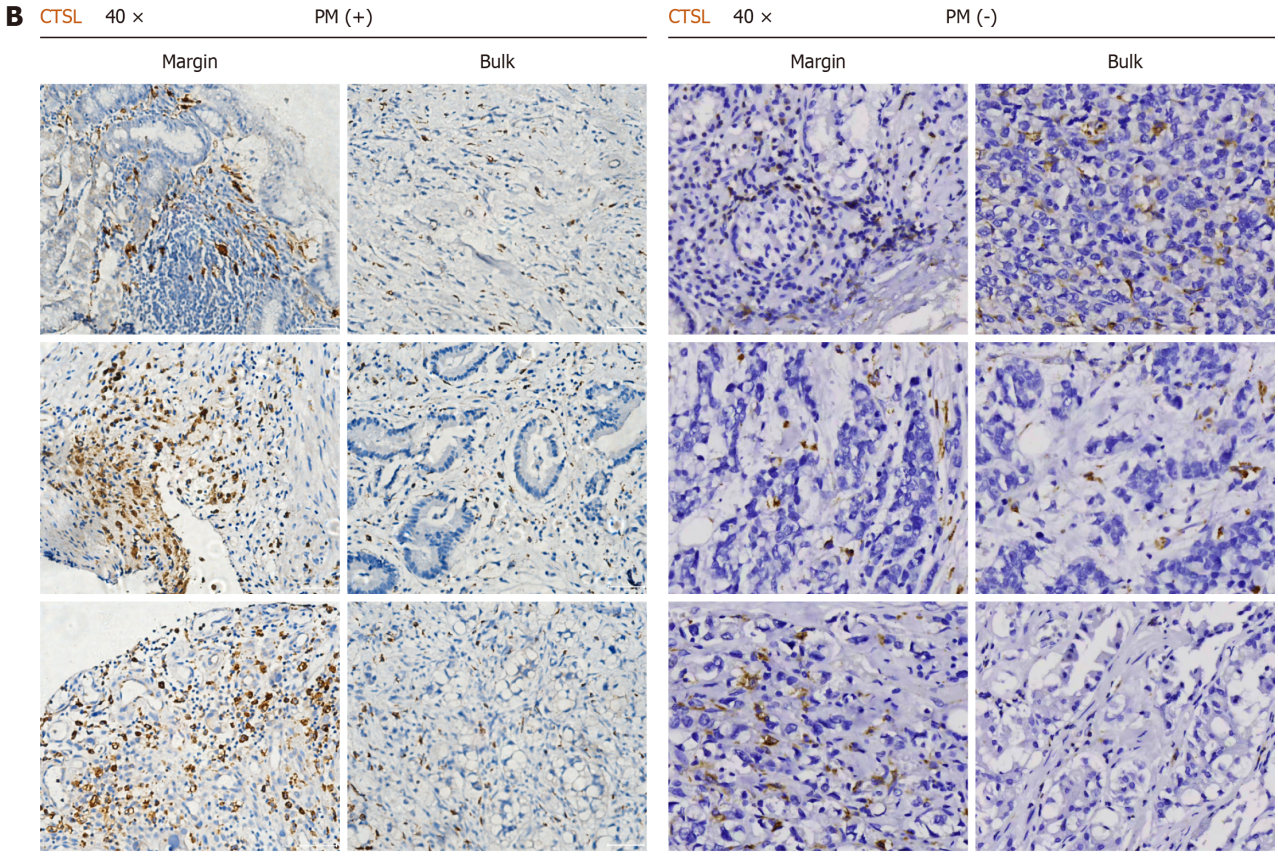
B
CTSL 40 ×
PM (+)
Margin
Bulk
CTSL 40 ×
PM (-)
Margin
Bulk

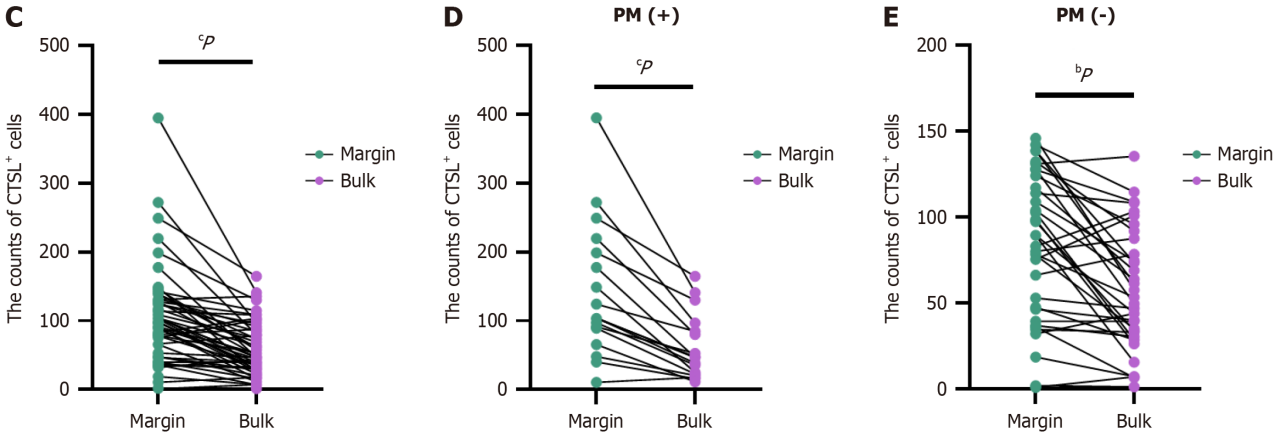
C
The counts of CTSL+ cells
500
400
300
200
100
0
cP
Margin
Bulk
Margin
Bulk
D
PM (+)
The counts of CTSL+ cells
500
400
300
200
100
0
cP
Margin
Bulk
Margin
Bulk
E
PM (-)
The counts of CTSL+ cells
200
150
100
50
0
bP
Margin
Bulk
Margin
Bulk

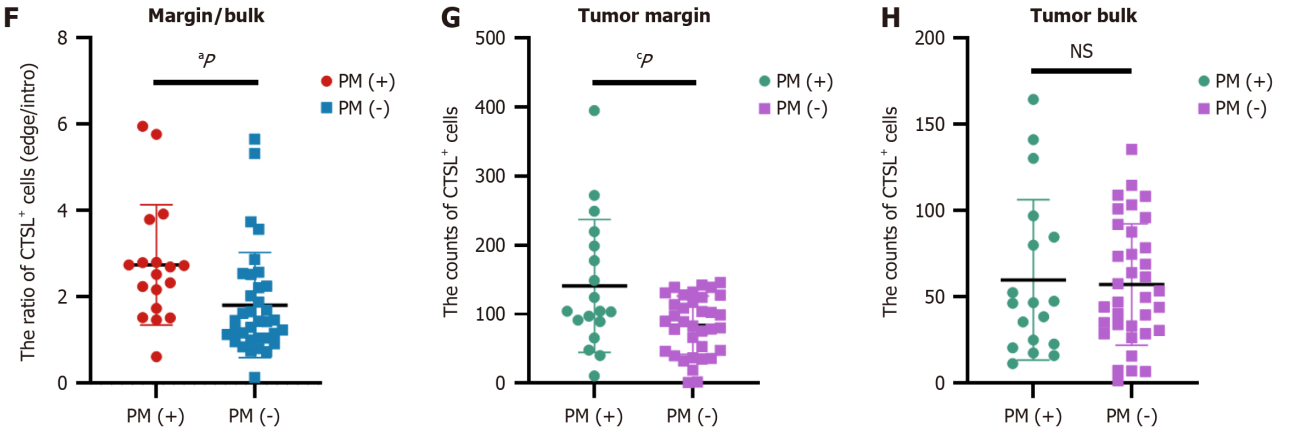

Figure 2 Cathepsin L is more localized in the gastric tumor margin than in the bulk. A: Example diagram of the method for classifying tumor sections stained for cytokeratin, which defines the 2-mm-wide area away from the edge of the tumor as the tumor margin; scale bar, 500 μm; B-E: Representative immunohistochemistry images of the margin and bulk of each tumor section from patients with or without peritoneal metastasis stained for cathepsin L; scale bar, 50 μm. The number of positive cells in the tumor sections was quantified *via* Image J *via* the geometric mean of 3 representative views from each section. The data points are presented as the means ± SD. The error bars represent the SD; $^{c}P < 0.001$; $^{b}P < 0.01$ according to Student's *t* test; F-H: Significant analysis of positive cell counts according to the metastasis state in the tumor margin or bulk region by Image J *via* the geometric mean of 3 representative views from each section. The data points are presented as the means ± SD. The error bars represent the SD; NS: Not significant, $P > 0.05$; $^{a}P < 0.05$; $^{c}P < 0.001$ according to Student's *t* test. CTSL: Cathepsin L; PM: Peritoneal metastasis.

To clarify the exact role of macrophage-derived CTSL in gastric tumor cells, we transfected lentiviral vectors into the human mononuclear cell line THP-1 to knock down CTSL molecules (Figure 3C). Furthermore, we selected MKN45 cells, a gastric tumor cell line with high expression levels of E-cadherin, and MGC803 cells, which have moderate expression of E-cadherin (Figure 3D), for coculture with CTSL^{KD} THP-1 cells. E-cadherin has been identified as a CTSS ubstrate and can be directly cleaved by CTSB, CTSL, and CTSS both *in vitro* and *in vivo*[7], leading to loss of cell-cell adhesion and thus enhancing tumor invasion *via* the expression of the transcription factor Snail[28]. For gastrointestinal malignancies, degradation of E-cadherin is required for EMT, resulting in a motile and invasive cellular phenotype[29]. Invasion and wound healing assays revealed that CTSL knockdown significantly inhibited the invasion and migration of gastric tumor cells (Figure 3E and F), suppressing tumor dissemination and metastasis.

Furthermore, we extracted proteins from gastric cells after coculture with CTSL^{KD} or shNC THP-1 cells and estimated the expression of EMT-related proteins. Decreases in E-cadherin, nuclear β-catenin, and p120 catenin are the most critical alterations during tumorigenesis[30], as cadherins are inseparably connected with catenins, which form a cadherin-catenin complex and contribute to cell-cell adhesion. The results revealed decreased E-cadherin and decreased levels of the transcriptional protein Snail and increased levels of N-cadherin and β-catenin (Figure 3G). As degradation or destabilization of the cadherin-catenin complex may result in tumor progression, macrophage-derived CTSL can improve the breakdown of the cadherin-catenin complex and result in tumor progression *in vitro*. However, we found that the inhibitory effects of CTSL knockdown on MGC803 cells were weaker than those on MKN45 cells, which may be due to the lower baseline E-cadherin expression level in the MGC803 cell line.

CTSL expression contributes to the M2-like polarization of macrophages in gastric tumors

TAMs mainly originate from circulating bone marrow hematopoietic stem cell-derived monocytes but can also evolve from tissue-resident cells[31,32]. In the chronological sequence of tumorigenesis, M1-like macrophages initially activate immune functions and exert antitumor effects, but the tumor microenvironment gradually subverts TAMs into tumor-promoting M2-like macrophages, which are enriched in hypoxic areas in the tumor bulk[33].

Classically activated macrophages (M1-like) and alternatively activated macrophages (M2-like) perform opposite functions in the TME. To further identify the role of CTSL, we performed multiplex immunohistochemical staining of M1-like macrophage markers and CTSL molecules. The results revealed strong overlap between CD163 (a marker of the M2 subtype) and CTSL in gastric cancer (Figure 4A and B); notably, the positive signals were mainly in the tumor margin region rather than in the "desert" tumor bulk (Figure 4C and D).

The high CTSL expression in M2-like macrophages in the gastric tumor margin supports the hypothesis that CTSL is associated with macrophage polarization. In the traditional binary classification, macrophages are broadly classified into the classically activated M1 subtype (proinflammatory), which is induced by lipopolysaccharide (LPS) or Th1 cytokines [interferon γ (IFN-γ), tumor necrosis factor-α (TNF-α)], or the alternatively activated M2 subtype (anti-inflammatory), which is induced by Th2 cytokines [interleukin (IL)-4, IL-13] *via* signal transducer and activator of transcription (STAT) 6 or IL-10 *via* STAT3 signaling[34]. As the first responders, macrophages recognize and bind pathogen-associated patterns such as LPS with surface Toll-like receptor 4 to activate transcription factors (interferon regulatory factors and nuclear factor kB) to drive inflammatory responses[35]. This proinflammatory M1 phenotype results in the release of various cytokines, such as IL-1β, IL-6, and TNF-α, improving the recruitment and infiltration of more macrophages and leukocytes. Meanwhile, M2 macrophages secrete large amounts of IL-10 and transforming growth factor-β to inhibit inflammation in the wounding environment, contributing to tissue repair, remodeling, and angiogenesis to control the

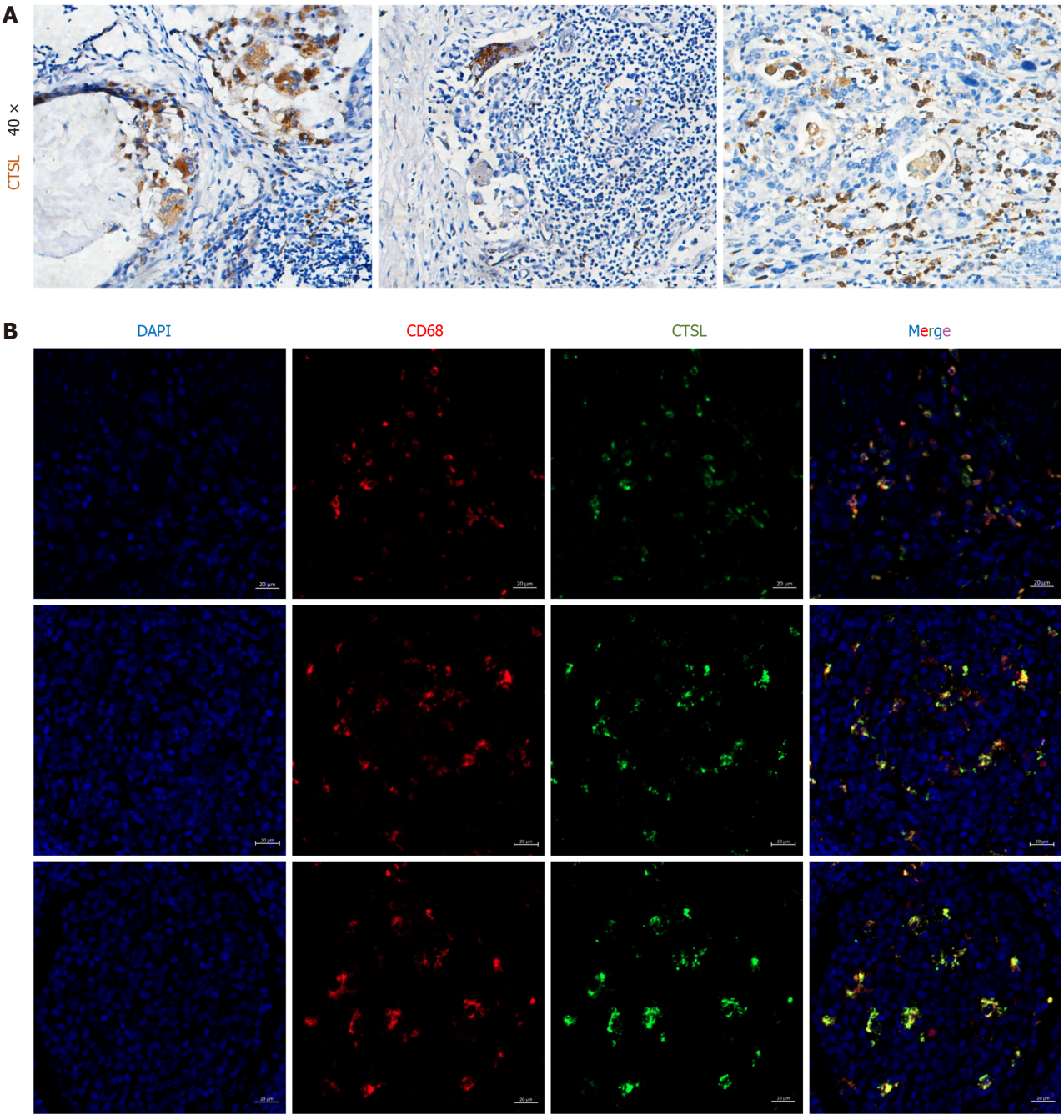
A
CTSL 40 ×
B
DAPI
CD68
CTSL
Merge
C
THP-1
dP
bP
NS
Relative mRNA expression of CTSL
1.5
1.0
0.5
0.0
shCTSL1
shCTSL2
shNC
NC
THP-1
shCTSL1
shCTSL2
shNC
NC
CTSL
38 kda
β-actin
43 kda
D
SNU 216
MGC 803
MKN 45
HGC 27
SGC 7901
BGC 823
NCC 24
AGS
E-cadherin
120 kda
β-actin
43 kda

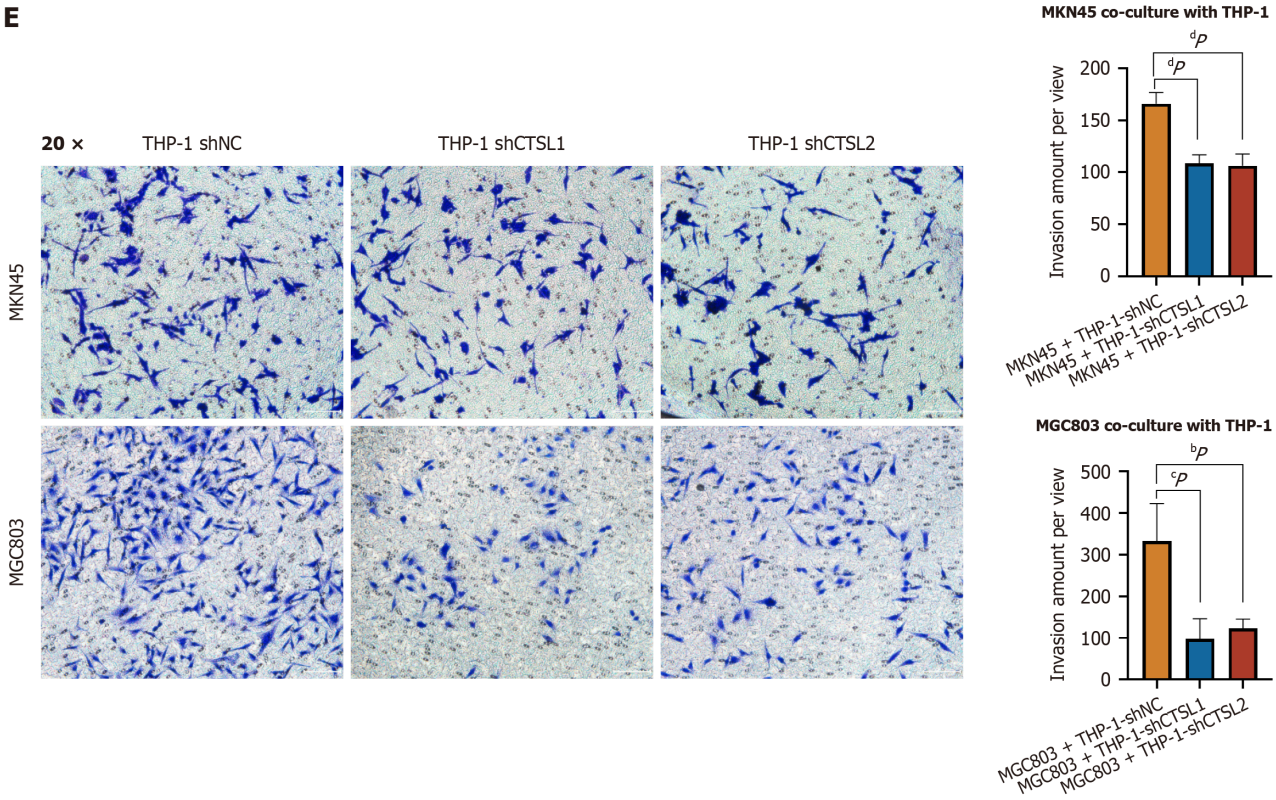
E
20 ×
THP-1 shNC
THP-1 shCTSL1
THP-1 shCTSL2
MKN45
MGC803
MKN45 co-culture with THP-1
Invasion amount per view
200
150
100
50
0
dP
dP
MKN45 + THP-1-shNC
MKN45 + THP-1-shCTSL1
MKN45 + THP-1-shCTSL2
MGC803 co-culture with THP-1
Invasion amount per view
500
400
300
200
100
0
bP
cP
MGC803 + THP-1-shNC
MGC803 + THP-1-shCTSL1
MGC803 + THP-1-shCTSL2

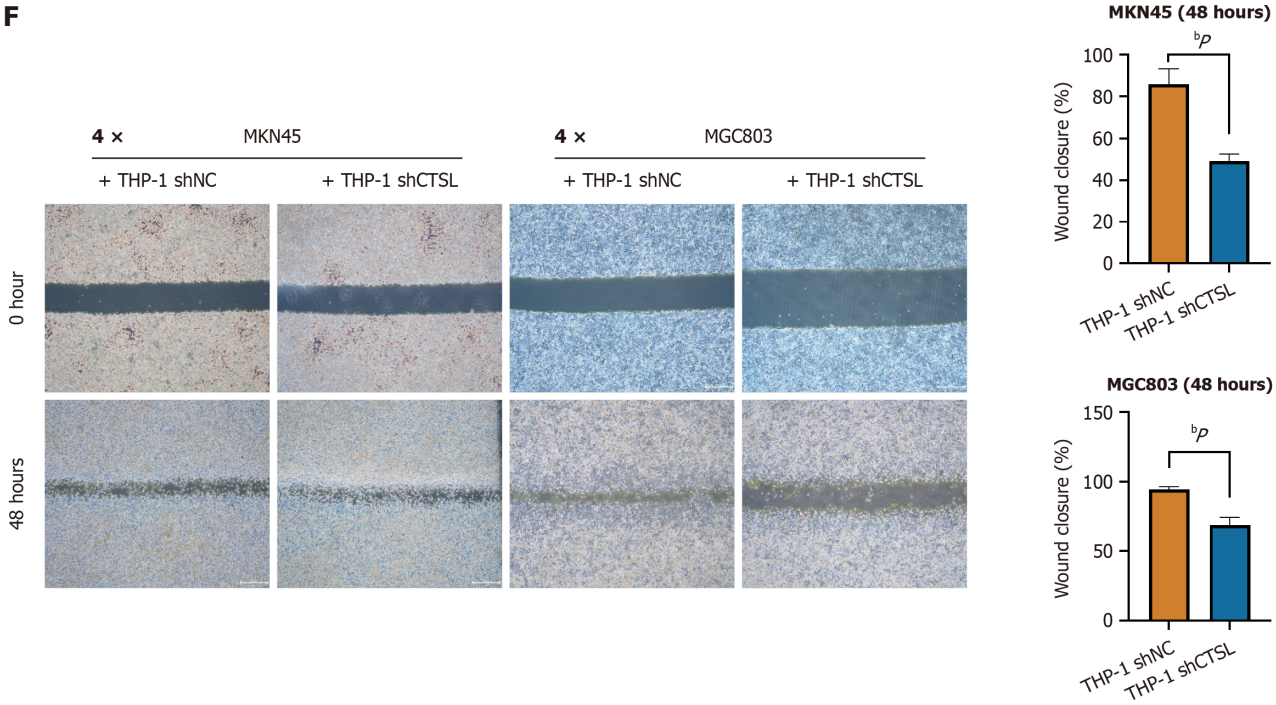
F
4 ×
MKN45
+ THP-1 shNC
+ THP-1 shCTSL
4 ×
MGC803
+ THP-1 shNC
+ THP-1 shCTSL
0 hour
48 hours
MKN45 (48 hours)
Wound closure (%)
100
80
60
40
20
0
bP
THP-1 shNC
THP-1 shCTSL
MGC803 (48 hours)
Wound closure (%)
150
100
50
0
bP
THP-1 shNC
THP-1 shCTSL

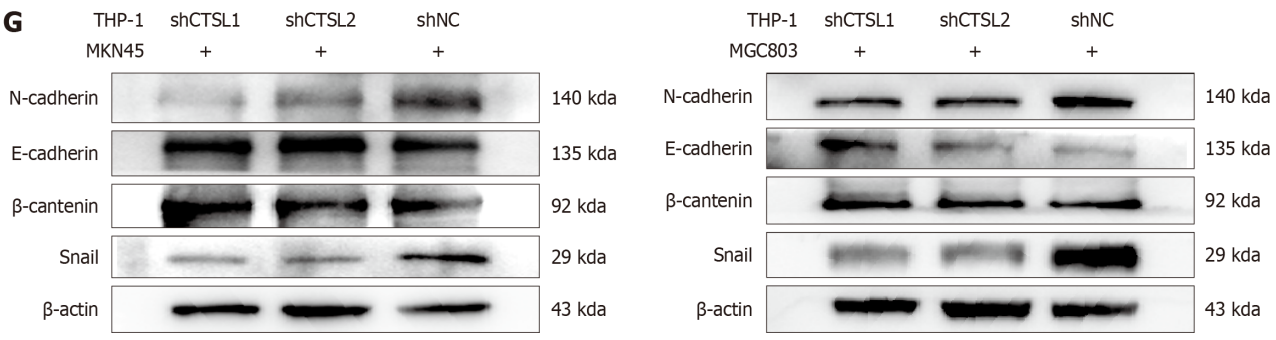
G
THP-1
shCTSL1
shCTSL2
shNC
MKN45
+
+
+
N-cadherin
E-cadherin
β-cantenin
Snail
β-actin
140 kda
135 kda
92 kda
29 kda
43 kda
THP-1
shCTSL1
shCTSL2
shNC
MGC803
+
+
+
N-cadherin
E-cadherin
β-cantenin
Snail
β-actin
140 kda
135 kda
92 kda
29 kda
43 kda

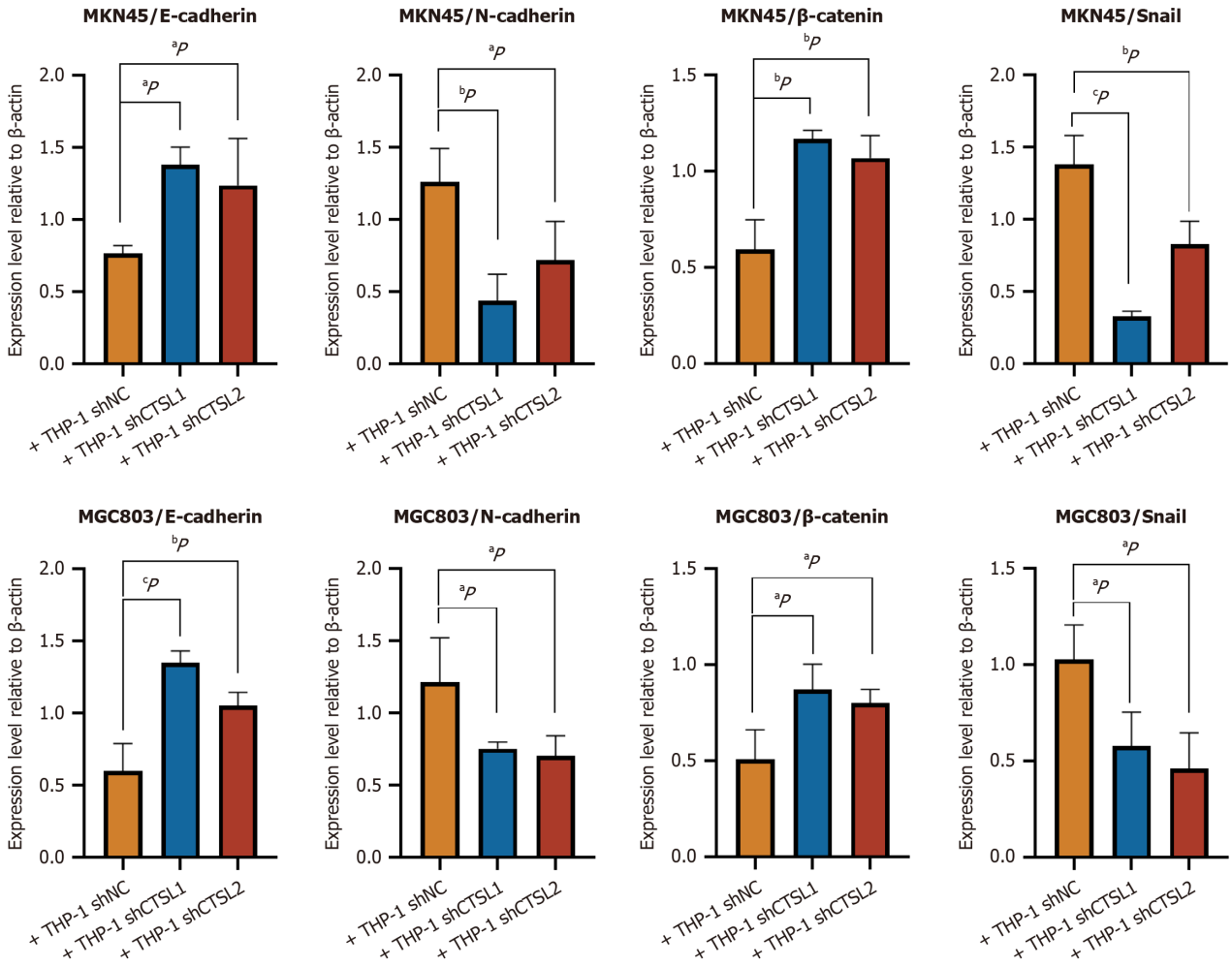

Figure 3 Cathepsin L is critical for macrophages to promote gastric tumor invasion and migration *via* epithelial-mesenchymal transition. A: Representative immunohistochemistry images of multinucleated giant cells stained for cathepsin L (CTSL) in gastric tumor sections. Magnification, 40 ×; B: Immunofluorescence analysis of CTSL and CD68 in the tumor tissue of gastric cancer patients; scale bar, 20 mm; C: The qPCR and Western blot analysis of shCTSL-treated THP-1 cells. The error bars represent the SD; NS: $P > 0.05$; $^{c}P < 0.001$; $^{b}P < 0.01$ according to one-way analysis of variance (ANOVA); D: Invasion assay of the gastric cancer cell lines MKN45 and MGC803 cocultured with shCTSL or shNC THP-1 cells. Magnification, 20 ×. The chemotactic cells that migrated through the Matrigel in the five views of each group were quantified manually. The error bars represent the SD; $^{b}P < 0.01$; $^{c}P < 0.001$; $^{d}P < 0.0001$ according to one-way ANOVA; E: Wound healing assay of the gastric cancer cell lines MKN45 and MGC803 cocultured with shCTSL or shNC THP-1 cells for 48 hours. Magnification, 4 ×. The wound closure area was quantified *via* Image J *via* data from 3 independent experiments. The error bars represent the SD; $^{b}P < 0.01$; according to Student's *t* test; F: Western blot analysis of E-cadherin levels in various gastric cancer cell lines; G: Western blot analysis of epithelial-mesenchymal transition-related proteins (E-cadherin, β-catenin, N-cadherin, and Snail) in MKN45 and MGC803 cells cocultured with shCTSL or shNC-transfected THP-1 cells for 48 hours. Blots from three independent experiments were quantified *via* Image J. The error bars represent the SD; $^{c}P < 0.001$; $^{b}P < 0.01$; $^{a}P < 0.05$ according to one-way ANOVA. CTSL: Cathepsin L; DAPI: 4',6-diamidino-2-phenylindole.

overactive immune response[36].

Moreover, the polarization of macrophages has been reported to be associated with EMT in fibrosis and tumor progression. In fibrosis-related diseases, M2 macrophage polarization can promote peritoneal fibrosis[37], tubulointerstitial fibrosis[38], and chronic obstructive pulmonary disease[39] *via* the modulation of EMT. The EMT of endometrial epithelial cells can also be accelerated by inducing M2-like macrophage polarization[40]. With respect to neoplasms, miR-98 was reported to suppress the TAM-induced promotion of the EMT and invasion of hepatocellular carcinoma by modulating macrophage polarization[41]. In addition, the inhibition of several bioactive molecules can induce EMT and M2 macrophage polarization simultaneously and further intervene in the course of tumors and fibrosis. For example, enhancer of zeste homolog 2 promotes renal fibrosis by inducing EMT and M2 macrophage polarization[42]. Histone deacetylase 8 inhibition prevents peritoneal fibrosis by counteracting EMT and blocking M2 macrophage polarization [43]. LCZ696, an angiotensin receptor-neprilysin inhibitor, can ameliorate the EMT of peritoneal mesothelial cells and M2 macrophage polarization[44].

We induced THP-1 cells to the M0 state *in vitro* for IF staining and detected a low level of CD163 in CTSL^{KD} THP-1 cells, but no significant difference in CD86 (a marker of the M1 subtype) expression was found compared with that in normal M0-state THP-1 cells (Figure 4E). Next, M0-state macrophages were induced into the M1 state by LPS and IFN-γ and induced into the M2 state by IL-4 and IL-13[34,45]. The qRT-PCR revealed decreased expression of M2 markers (CD163, CD206, IL-10, and arginase 1) and increased expression of M1 markers (TNF-α and IL-6) in CTSL^{KD} macrophages

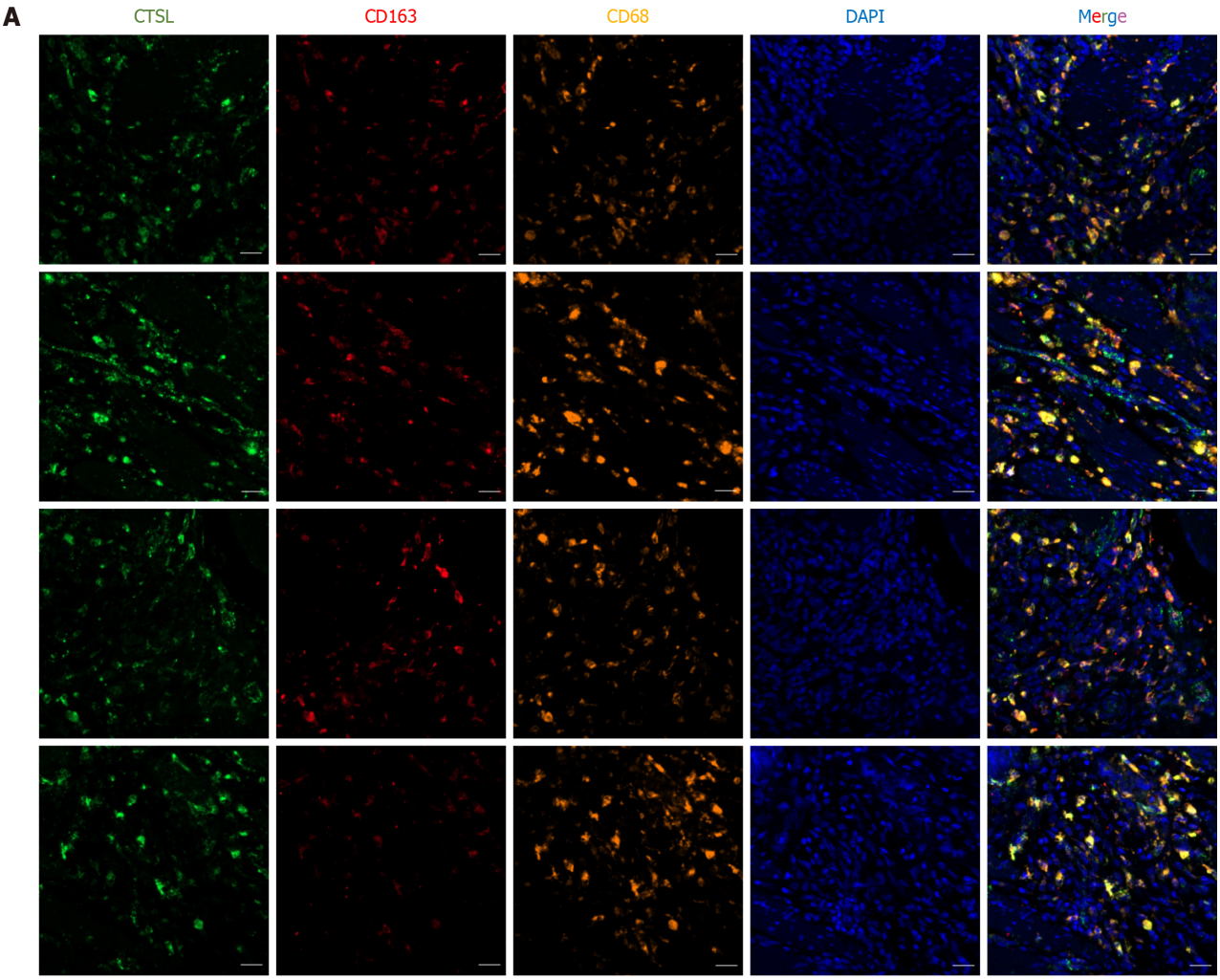
A
CTSL
CD163
CD68
DAPI
Merge

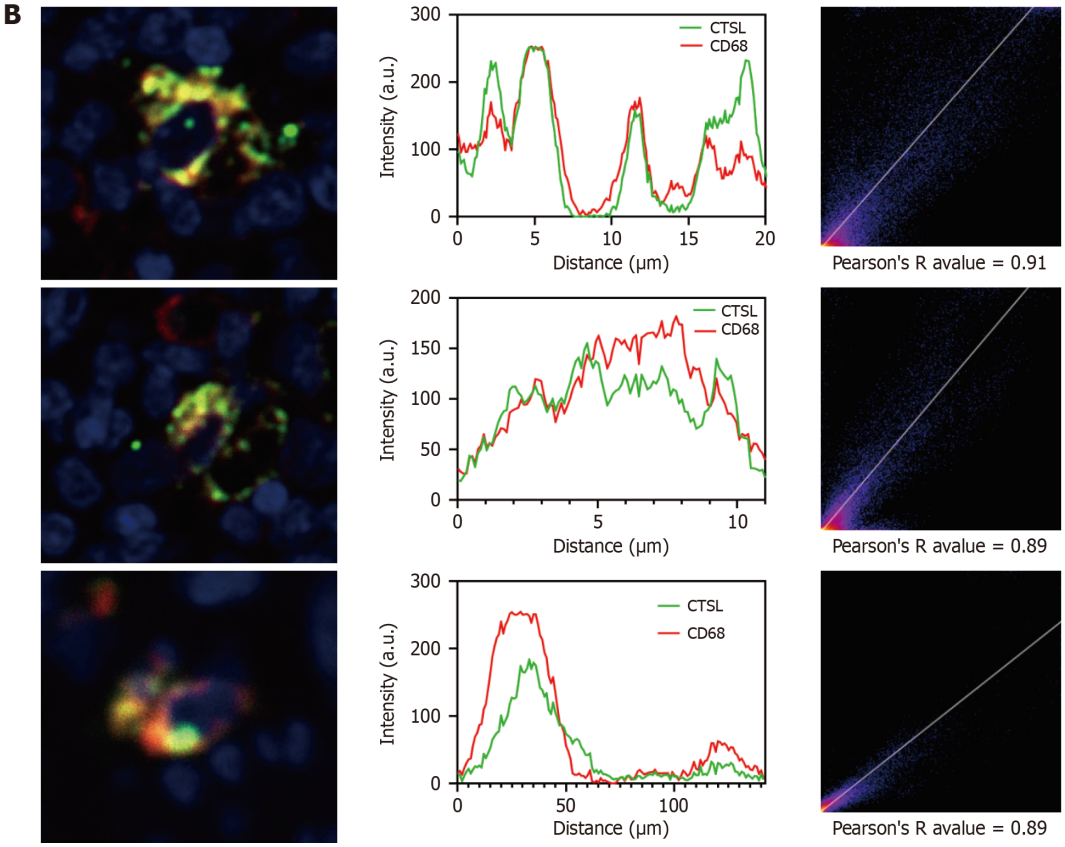
B
CTSL
CD68
Intensity (a.u.)
Distance (μm)
Pearson's R avalue = 0.91
Pearson's R avalue = 0.89
Pearson's R avalue = 0.89

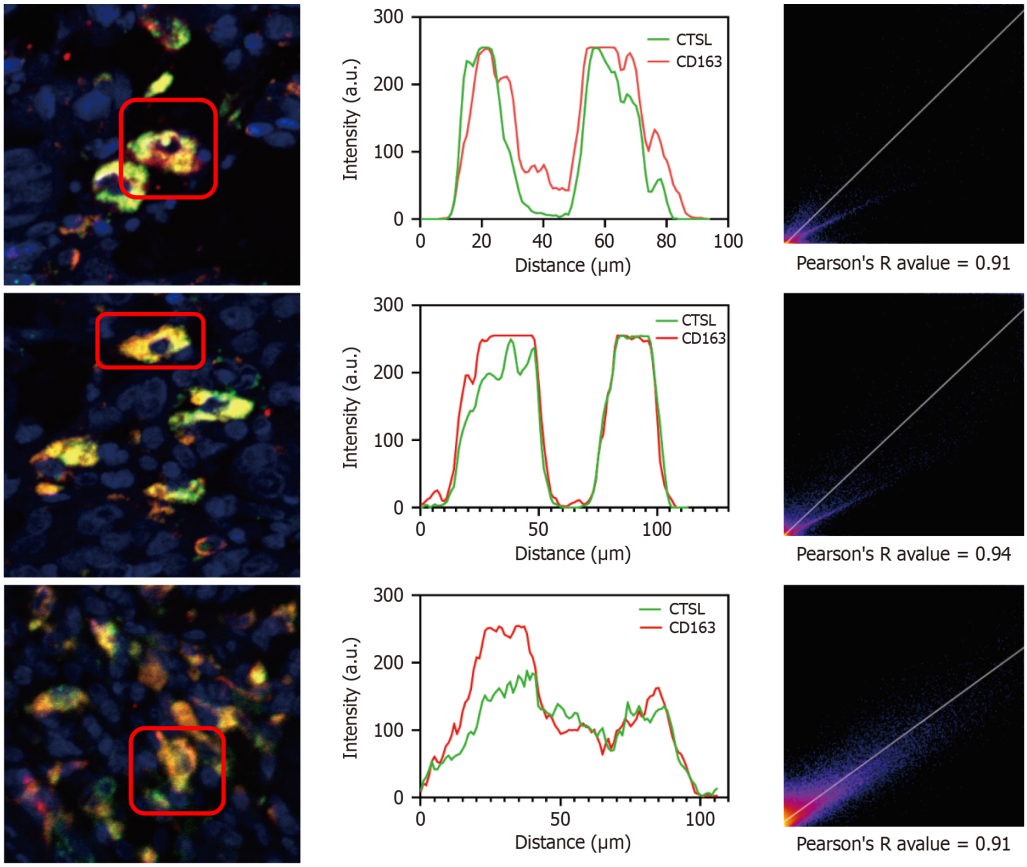
CTSL
CD163
Intensity (a.u.)
Distance (μm)
Pearson's R avalue = 0.91
Pearson's R avalue = 0.94
Pearson's R avalue = 0.91

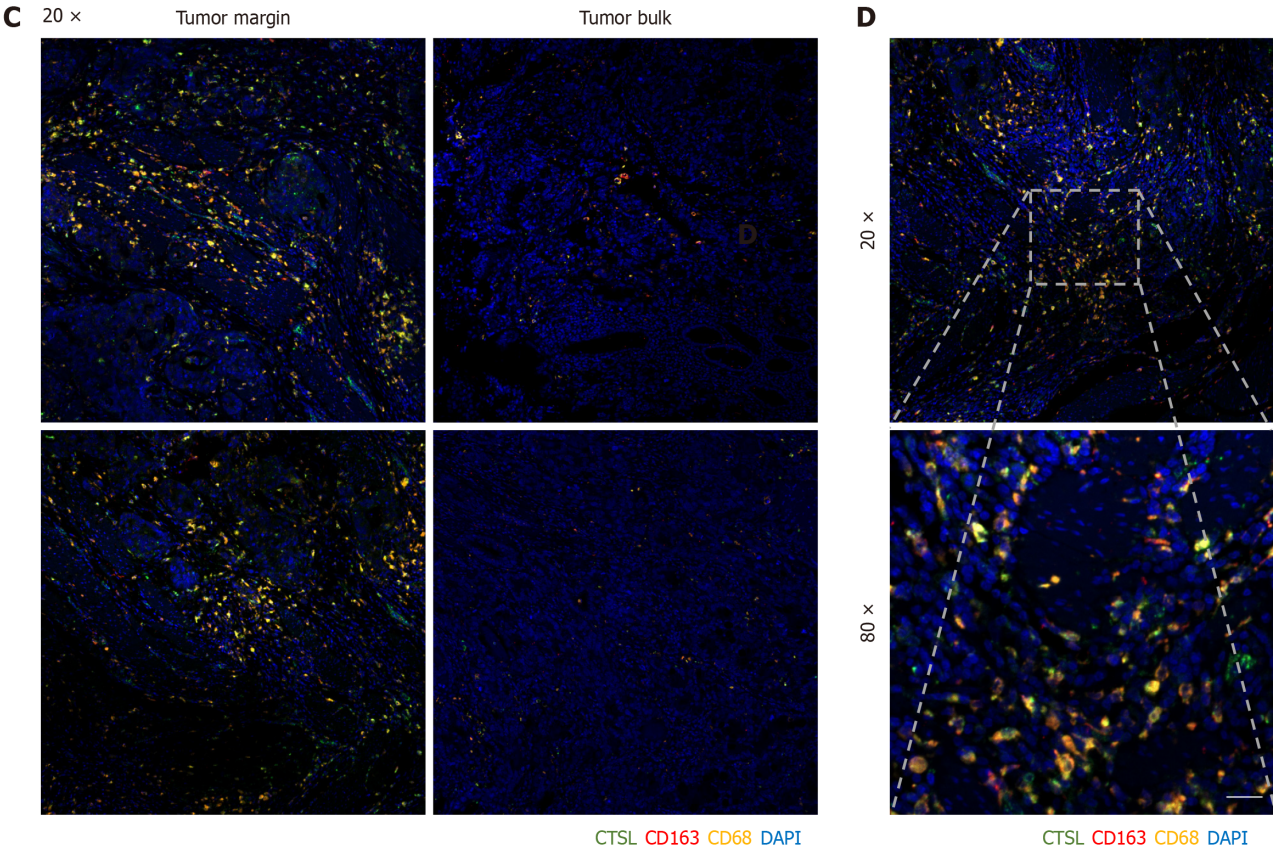
C
20 ×
Tumor margin
Tumor bulk
D
20 ×
80 ×
CTSL CD163 CD68 DAPI
CTSL CD163 CD68 DAPI

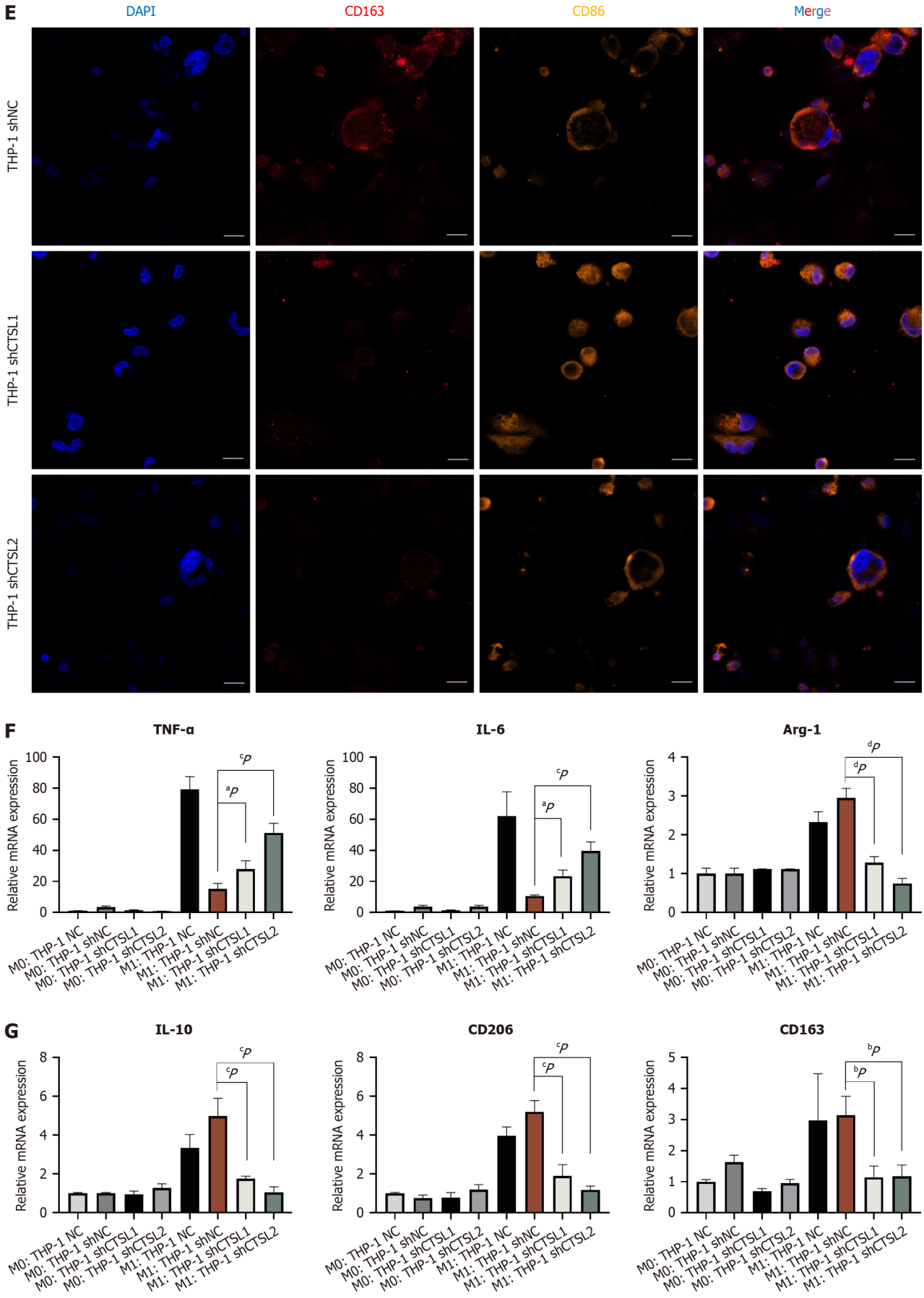

Figure 4 Cathepsin L + macrophages exert orienting effects on polarization. A: Multiplied immunohistochemistry (mIHC) analysis of cathepsin L (CTSL), CD68, and CDD163 in human gastric tumor sections; scale bar, 20 μm; B: Correlation analysis between CTSL and macrophage markers (CD68 or CD163)

via Pearson's R value measured by Image J; |R| ≤ 1; C and D: Representative mIHC images stained for CTSL, CD68, and CD163 in the tumor margin and bulk of human gastric tissues; magnification, 20 ×, 80 ×; E: Immunofluorescence analysis of CD163 and CD86 expression in shCTSL-transfected or shNC-transfected THP-1 cells; scale bar, 20 μm; F: Quantitative real-time polymerase chain reaction analysis of mRNAs extracted from shCTSL-treated or shNC-treated macrophages induced into the M0/M1/M2 state *in vitro*; the results revealed increased M1 and decreased M2 marker mRNA levels in shCTSL-treated macrophages. The error bars represent the SD; $^{c}P < 0.001$; $^{b}P < 0.01$; $^{a}P < 0.05$ according to one-way analysis of variance. CTSL: Cathepsin L; DAPI: 4',6-diamidino-2-phenylindole; TNF-α: Tumor necrosis factor-α; IL: Interleukin; Arg-1: Arginase 1.

(Figure 4F), suggesting that CTSL is positively related to M2-like phenotype expression. These results revealed that CTSL likely contributes to M2-like polarization, indirectly contributing to gastric cancer progression.

Macrophage-derived CTSL accelerates gastric tumor invasion and dissemination via EMT in vivo

To further verify the protumoral effects of macrophage-derived CTSL, we established a murine model with subcutaneous tumors *in vivo*. On the basis of the results of the animal study, we found that macrophage-derived CTSL can promote tumor growth and EMT progression in gastric cancer. In this study, MKN45 gastric cells were injected with THP-1 cells or $CTSL^{KD}$ THP-1 cells subcutaneously into 4-week-old male BALB/c nude mice (Figure 5A). By measuring the tumor growth volume and weight, we observed that MKN45 gastric cells and shNC-treated THP-1 cells grew faster than did $CTSL^{KD}$-treated THP-1 cells. The tumor volume in the $CTSL^{KD}$ group was significantly smaller than that in the control group ($n = 5$, $^{a}P < 0.05$) (Figure 5B-D), indicating the stimulating effects of CTSL on gastric cancer cell growth *in vivo*. The IHC results revealed that the tumors of MKN45 cells mixed with shNC THP-1 cells presented lower expression of the EMT critical molecule E-cadherin than did those of MKN45 cells mixed with $CTSL^{KD}$ THP-1 cells (Figure 5E), supporting our *in vitro* findings that macrophage-derived CTSL can increase the expression of E-cadherin and promote the EMT progression of gastric cancers. The effectiveness of the injected tumor cells was confirmed by HE and immunohistochemical staining for Ki67, and the presence of macrophages was detected *via* CD68 staining (Figure 5E).

Despite varying results in animal models, the subcutaneous mouse model is not good enough to imitate the *in vivo* tumor microenvironment of gastric cancer in humans, which deserves further optimization and in-depth study. However, analogous findings may also exist in colorectal carcinoma considering the similarity of gastrointestinal tumors.

DISCUSSION

Gastric cancer peritoneal metastasis (GCPM) is prevalent in patients with advanced gastric cancer and is associated with a dismal prognosis and limited therapies. Multiple studies have examined certain locoregional (intraperitoneal) treatments, including intraperitoneal (IP) chemotherapy, hyperthermic IP chemotherapy, and pressurized intraperitoneal aerosol chemotherapy (PIPAC), which can be prospective treatment options for refractory PMs of various origins[46–48], but the response of PMs to systemic antineoplastic therapy is still limited due to the presence of the peritoneal-plasma barrier and poor cancer tissue vascularity. To identify promising target molecules, we explored the molecular biology of GCPM further in this study. First, we observed increased CTSL expression in the tumor margins of gastric cancer patients with peritoneal metastasis through IHC and IF analysis. Second, owing to the high overlap of CTSL and macrophage markers in the TME, we constructed stable $CTSL^{KD}$ THP-1-derived macrophages *via* lentiviral infection and examined the effects of CTSL on macrophage polarization. By coculturing macrophages and gastric tumor cells *in vitro* and *in vivo*, we demonstrated that macrophage-derived CTSL promote gastric tumor invasion and metastasis. Our findings indicate that immunotherapy targeting macrophages may facilitate GCPM treatment.

Histologically, the peritoneum is composed of monolayer mesothelial cells with a basement membrane laid on connective tissues. The exact reason why peritoneal tissue is a preferential site for the metastasis of intraperitoneal tumors is still unknown, but it has been reported to be associated with omental 'milky spots' containing abundant immune aggregates and capillary networks[49,50], where macrophages are the primary components of leukocytes[51]. Like the distribution of the cathepsin proteinase, macrophages within the tumor microenvironment are frequently observed at the break of the basement membrane in the early stage of malignant transformation and at the invasive front of advanced tumors, improving angiogenesis and ECM degradation and remodeling[26,52]. The remodeling capacity of macrophages enables cancer cells to access and migrate through the surrounding stroma[36,53], paving the way for the first step of tumor metastasis. Tumor-associated macrophages have also been reported to promote PM through the secretion of IL-6 [54]. In addition, macrophages also produce multiple chemicals, including mutagenic oxygen, nitrogen radicals, and angiogenic factors, contributing to tumor initiation and progression[53]. Notably, Gocheva *et al*[55] demonstrated that IL-4 increases the activity of CTSB and S in macrophages *in vitro* and *in vivo*, promoting pancreatic tumor angiogenesis, growth, and invasion. Shree *et al*[56] reported that cathepsin-expressing macrophages protect against taxol-induced tumor cell death and thus blunt the chemotherapeutic response in breast cancer partially *via* CTSB and CTSS. However, no reports regarding the role of macrophage-derived cathepsins in gastric cancer have been published. Although our study did not cover the 'milky spots' in omental tissue due to the lack of an ideal *in vivo* model, we found that macrophages promoted E-cadherin degradation and the EMT process by secreting CTSL, which significantly improved gastric tumor cell invasion and migration.

Primary gastric tumors with the EMT phenotype develop peritoneal metastasis more frequently and have a worse prognosis than all non-EMT subtypes do[57]. Downregulated intercellular adhesion molecules, especially typical cadherins, such as E-cadherin, have been demonstrated to be associated with EMT and PC[58]. The extracellular domain

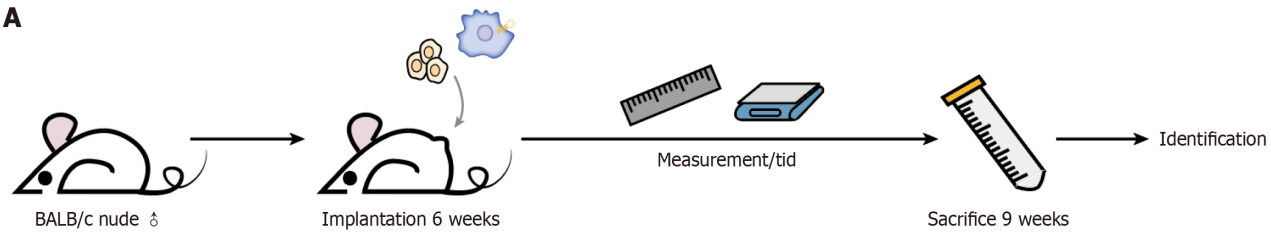
A
BALB/c nude
Implantation 6 weeks
Measurement/tid
Sacrifice 9 weeks
Identification

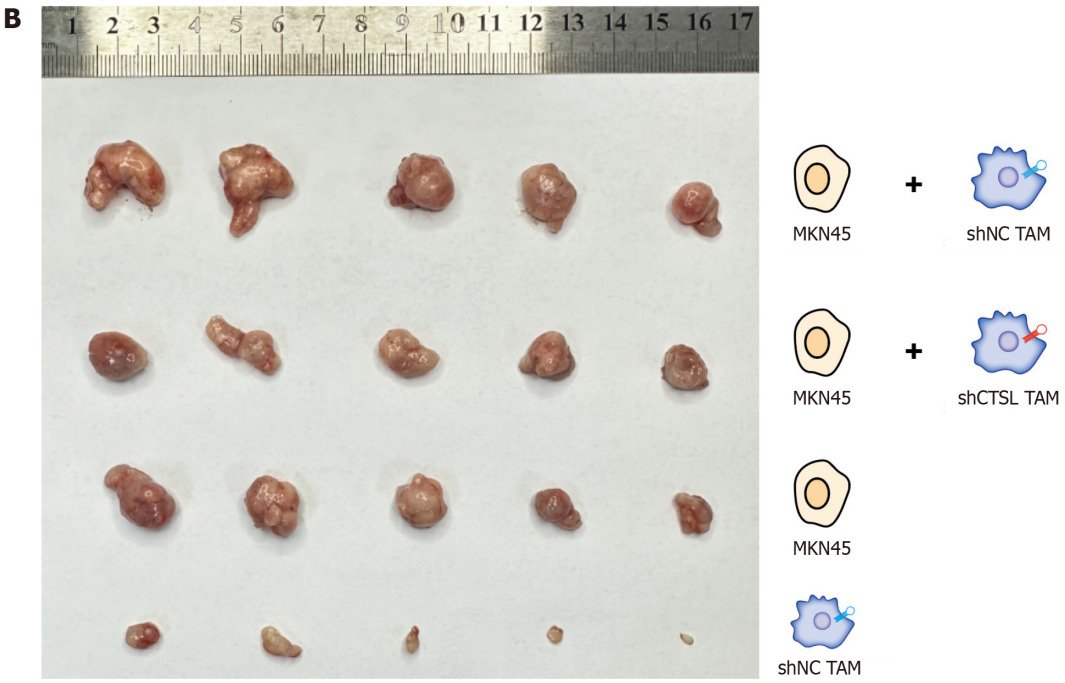
B
MKN45
shNC TAM
MKN45
shCTSL TAM
MKN45
shNC TAM

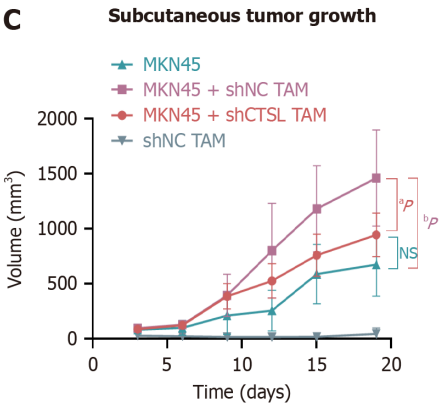
C
Subcutaneous tumor growth
MKN45
MKN45 + shNC TAM
MKN45 + shCTSL TAM
shNC TAM
Volume (mm3)
Time (days)
aP
bP
NS

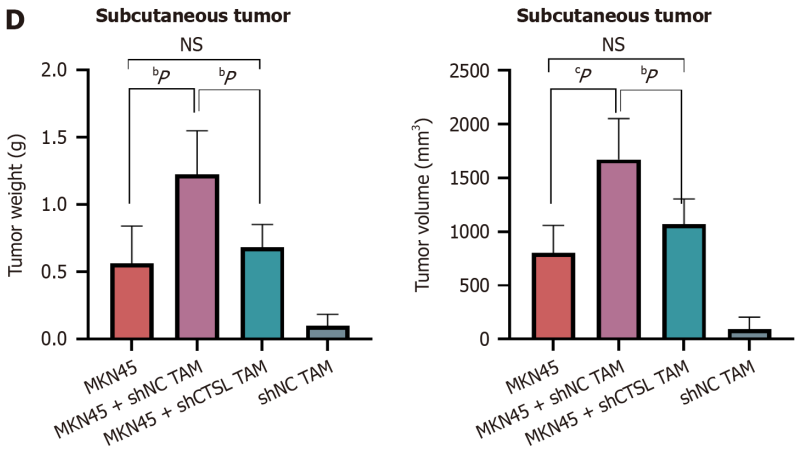
D
Subcutaneous tumor
Tumor weight (g)
Tumor volume (mm3)
NS
bP
cP
MKN45
MKN45 + shNC TAM
MKN45 + shCTSL TAM
shNC TAM

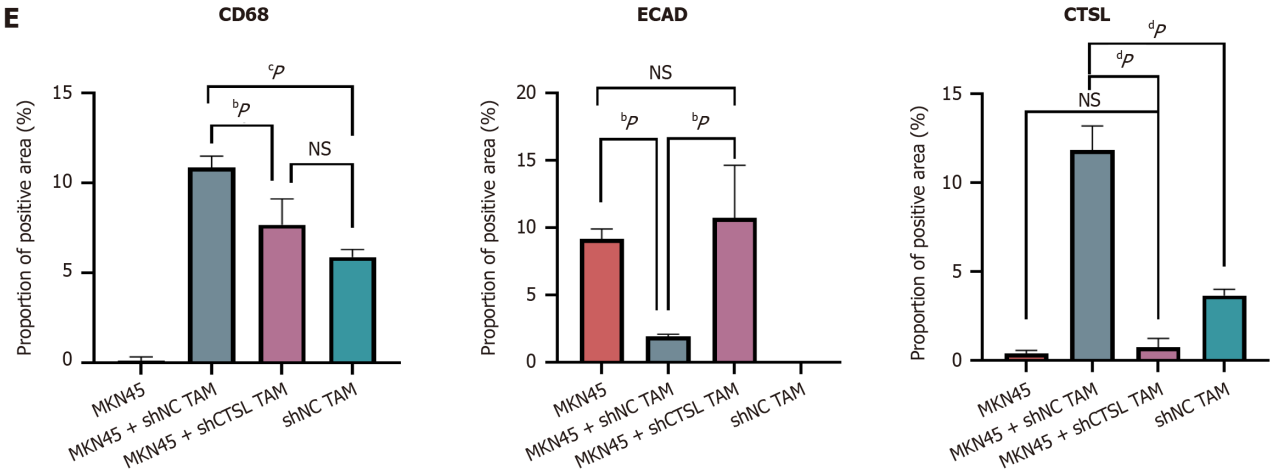
E
CD68
ECAD
CTSL
Proportion of positive area (%)
NS
bP
cP
dP
MKN45
MKN45 + shNC TAM
MKN45 + shCTSL TAM
shNC TAM

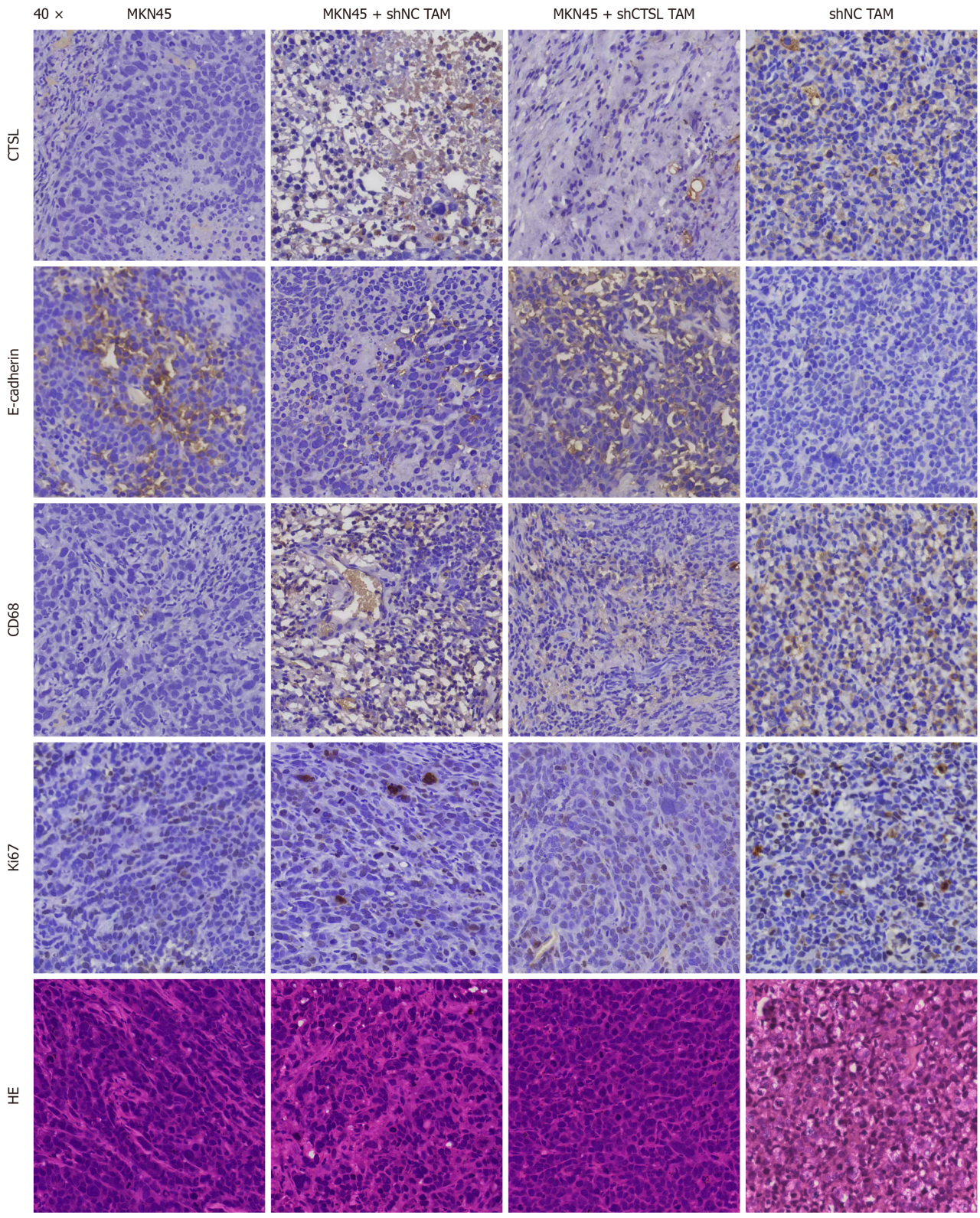

Figure 5 Cathepsin L knockdown impairs macrophage-induced gastric cancer tumorigenesis *in vivo*. A: Experimental design of the animal study. Wild type male BALB/c nude mice had MKN45 cells implanted into the subcutaneous space and were mixed with either sh cathepsin L (CTSL) or shNC tumor-associated macrophage (TAM); B: Morphological characteristics of tumors in the MKN45 + shNC TAM, MKN45 + shCTSL TAM, MKN45 alone, and shNC TAM groups; C: Volume of tumor growth at the indicated time points over 3 days. The error bars represent the SD; D: Tumor weight and volume *ex vivo*. The error bars represent the SD. $^{b}P < 0.01$; $^{a}P < 0.05$ according to one-way analysis of variance (ANOVA); E: Immunohistochemistry analysis of mouse tumor sections from different groups stained for CTSL, E-cadherin, CD68, and Ki67 proteins. Magnification, 40 ×. Quantification of E-cadherin, CTSL, and CD68 protein expression was performed *via* Image J. The error bars represent the SD. NS: Not significant, $P > 0.05$; $^{a}P < 0.05$; $^{b}P < 0.01$; $^{c}P < 0.001$ according to one-way ANOVA. TAM: Tumor-associated macrophage; HE: Haematoxylin and eosin; CTSL: Cathepsin L.

of E-cadherin is degraded by CTSL proteolytically with diminished adhesive properties[7]. In terms of cell surface proteins, CTSL has proteolytic activity and degrades ECM components (collagen types I and IV, fibronectin, and laminin) by directly cleaving the matrix and basement membrane or inducing a proteolytic cascade of other proteases, such as MMPs and urokinase[6,18]. Eventually, the degradation of E-cadherin can disrupt adherens junctions and favor tumor cell invasion and migration[6].

In addition, the relationship between CTSL and the M2 polarization of macrophages was verified in our study. We confirmed that $CTSL^{KD}$ THP-1-derived macrophages simultaneously express lower levels of M2-type markers and higher levels of M1-type markers. However, TAMs primarily exhibit M1-like or M2-like phenotypes instead of bona fide M1 or M2 binary subtypes in the variable tumor microenvironment[33,59]. Some subtypes of macrophages completely off the M1 and M2 spectrum also simultaneously exist within the tumor environment[45] and facilitate the maintenance of homeostasis *via* sophisticated crosstalk. Therefore, the effects of CTSL may be related to certain subgroups of macrophages under a more precise classification.

The incorporation of peritoneal-directed treatment with systemic therapy, in which more sophisticated intratumoral agents are delivered intraperitoneally through either PIPAC or other methods, has potential for future use in PM patients. For example, the effect of PIPAC-delivered oxaliplatin combined with systemic nivolumab in GCPM patients was assessed in the PIANO study (ClinicalTrials.gov identifier: No. NCT03172416)[60]. As decreased CTSL enables chemotherapeutic agents to reach the nucleus by reducing drug sequestration, the effectiveness of chemotherapy can also be enhanced through CTSL inhibition[61]. The results of our work show that CTSL inhibition not only prevents tumor invasion or metastasis through the suppression of EMT progression or the transfer of TAMs into the antitumor state but also may improve the therapeutic effects of chemotherapy on the basis of the function of CTSL itself. In this way, the primary choice for future therapy may be a medicine that targets CTSL on macrophages and applies intraperitoneal chemotherapy as a locoregional treatment. In addition, compared with targeted medicine, various CTSL inhibitors have more mature research and experimental development (R and D) systems, and some are derived from nature[62]. Li *et al* [63] discovered a selective a natural product CTSL inhibitor with antimetastatic ability *in vitro* and *in vivo* against breast cancer cells. The role of the CTSL inhibitor KGP94 in breast tumor angiogenesis and metastasis has also been examined [64,65]. Moreover, machine learning and artificial intelligence can be applied to discover novel CTSL inhibitors from natural products[66,67]. However, CTSL inhibitors have not been approved for clinical application. The unknown interaction between chemotherapy and inhibitors increases the potential risk of combination therapy.

However, some limitations still exist in our current study. First, the exact signal transduction mechanism of these protumor effects was not clarified in our study; thus, further studies on the specific effectors of macrophage-derived CTSL in the gastric tumor environment still need to be undertaken. Second, we used only two kinds of gastric cells because of the limited options for highly metastatic gastric cell lines. Third, we verified the *in vitro* results *via* subcutaneous tumors in BALB/c nude mice because of the technical difficulty in establishing a mouse model of peritoneal metastasis. The examination of a mature mouse model of PMs from gastric carcinoma *in situ* will be more convincing.

CONCLUSION

In conclusion, macrophage-derived CTSL can accelerate tumor invasion or metastasis by promoting epithelial-mesenchymal transition and M2 polarization in the gastric tumor microenvironment *in vitro* and *in vivo*. Considering the wide distribution and critical physiological functions of cathepsins throughout the body, inhibiting CTSL on macrophages with a precise delivery system to target the peritoneum might be a promising strategy for future clinical application.

FOOTNOTES

Author contributions: Li XJ, Xiao LX, Yu J, and Chen T were responsible for the concept and design; Yu J, Chen T, Qiu RJ, Zhai ZY, Fang CF, and Zhong W were responsible for the acquisition of data, providing animals, acquiring and managing patients, providing facilities; Xiao LX, Li XJ, Yu HY, Ding WF, and Zhu MS were responsible for analysis and interpretation of data, statistical analysis, biostatistics, and computational analysis; Xiao LX and Li XJ were responsible for writing, review, and revision of the manuscript; all of the authors read and approved the final version of the manuscript to be published.

Supported by The National Natural Science Foundation of China, No. 82272087 and No. 82103150; The Guangdong Natural Science Foundation Outstanding Youth Project, China, No. 2021B1515020055; and The Guangdong Provincial Key Laboratory of Precision Medicine for Gastrointestinal Cancer, China, No. 2020B121201004.

Institutional review board statement: The study was reviewed and approved by The Nanfang Hospital Institutional Review Board, No. NFEC-2021-008.

Institutional animal care and use committee statement: All procedures involving animals were reviewed and approved by The Institutional Animal Care and Use Committee of the Animal Ethics Committee of Nanfang Hospital, China, IACUC protocol number: No. IACUC-LAC-20230717-008.

Conflict-of-interest statement: The authors declare that they have no competing interests.

Data sharing statement: No additional data are available.

ARRIVE guidelines statement: The authors have read the ARRIVE guidelines, and the manuscript was prepared and revised according to the ARRIVE guidelines.

Country of origin: China

ORCID number: Lu-Xi Xiao 0000-0003-4995-5628; Wu Zhong 0000-0001-5607-471X; Tao Chen 0000-0003-1306-6538; Jiang Yu 0000-0003-0086-1604.

S-Editor: Luo ML
L-Editor: A
P-Editor: Zheng XM

REFERENCES

1 **Cortés-Guiral D**, Hübner M, Alyami M, Bhatt A, Ceelen W, Glehen O, Lordick F, Ramsay R, Sgarbura O, Van Der Speeten K, Turaga KK, Chand M. Primary and metastatic peritoneal surface malignancies. *Nat Rev Dis Primers* 2021; **7**: 91 [PMID: 34916522 DOI: 10.1038/s41572-021-00326-6]
2 **Koemans WJ**, Luijten JCHBM, van der Kaaij RT, Grootscholten C, Snaebjornsson P, Verhoeven RHA, van Sandick JW. The metastatic pattern of intestinal and diffuse type gastric carcinoma - A Dutch national cohort study. *Cancer Epidemiol* 2020; **69**: 101846 [PMID: 33126042 DOI: 10.1016/j.canep.2020.101846]
3 **Garg M**. Emerging roles of epithelial-mesenchymal plasticity in invasion-metastasis cascade and therapy resistance. *Cancer Metastasis Rev* 2022; **41**: 131-145 [PMID: 34978017 DOI: 10.1007/s10555-021-10003-5]
4 **Lankelma JM**, Voorend DM, Barwari T, Koetsveld J, Van der Spek AH, De Porto AP, Van Rooijen G, Van Noorden CJ. Cathepsin L, target in cancer treatment? *Life Sci* 2010; **86**: 225-233 [PMID: 19958782 DOI: 10.1016/j.lfs.2009.11.016]
5 **Chung SM**. Variant cathepsin L activity from gastric cancer tissue. *Jpn J Cancer Res* 1990; **81**: 813-819 [PMID: 2118894 DOI: 10.1111/j.1349-7006.1990.tb02650.x]
6 **Gocheva V**, Joyce JA. Cysteine cathepsins and the cutting edge of cancer invasion. *Cell Cycle* 2007; **6**: 60-64 [PMID: 17245112 DOI: 10.4161/cc.6.1.3669]
7 **Gocheva V**, Zeng W, Ke D, Klimstra D, Reinheckel T, Peters C, Hanahan D, Joyce JA. Distinct roles for cysteine cathepsin genes in multistage tumorigenesis. *Genes Dev* 2006; **20**: 543-556 [PMID: 16481467 DOI: 10.1101/gad.1407406]
8 **Rousselet N**, Mills L, Jean D, Tellez C, Bar-Eli M, Frade R. Inhibition of tumorigenicity and metastasis of human melanoma cells by anti-cathepsin L single chain variable fragment. *Cancer Res* 2004; **64**: 146-151 [PMID: 14729618 DOI: 10.1158/0008-5472.can-03-1717]
9 **Rofstad EK**, Mathiesen B, Kindem K, Galappathi K. Acidic extracellular pH promotes experimental metastasis of human melanoma cells in athymic nude mice. *Cancer Res* 2006; **66**: 6699-6707 [PMID: 16818644 DOI: 10.1158/0008-5472.CAN-06-0983]
10 **Farinati F**, Herszényi L, Plebani M, Carraro P, De Paoli M, Cardin R, Roveroni G, Rugge M, Nitti D, Grigioni WF, D'Errico A, Naccarato R. Increased levels of cathepsin B and L, urokinase-type plasminogen activator and its inhibitor type-1 as an early event in gastric carcinogenesis. *Carcinogenesis* 1996; **17**: 2581-2587 [PMID: 9006092 DOI: 10.1093/carcin/17.12.2581]
11 **Dohchin A**, Suzuki JI, Seki H, Masutani M, Shiroto H, Kawakami Y. Immunostained cathepsins B and L correlate with depth of invasion and different metastatic pathways in early stage gastric carcinoma. *Cancer* 2000; **89**: 482-487 [PMID: 10931446]
12 **Pan T**, Jin Z, Yu Z, Wu X, Chang X, Fan Z, Li F, Wang X, Li Z, Zhou Q, Li J, Liu B, Su L. Cathepsin L promotes angiogenesis by regulating the CDP/Cux/VEGF-D pathway in human gastric cancer. *Gastric Cancer* 2020; **23**: 974-987 [PMID: 32388635 DOI: 10.1007/s10120-020-01080-6]
13 **Yan Q**, Ertao Z, Zhimei Z, Weigang D, Jianjun P, Jianhui C, Chuangqi C. Systemic immune-inflammation index (SII): A More Promising Inflammation-Based Prognostic Marker for Patients with synchronic colorectal peritoneal carcinomatosis. *J Cancer* 2020; **11**: 5264-5272 [PMID: 32742472 DOI: 10.7150/jca.46446]
14 **Wesselink E**, Boshuizen HC, van Lanen AS, Kok DE, Derksen JWG, Smit KC, de Wilt JHW, Koopman M, May AM, Kampman E, van Duijnhoven FJB; COLON and PLCRC studies. Dietary and lifestyle inflammation scores in relation to colorectal cancer recurrence and all-cause mortality: A longitudinal analysis. *Clin Nutr* 2024; **43**: 2092-2101 [PMID: 39094474 DOI: 10.1016/j.clnu.2024.07.028]
15 **Jaroenlapnopparat A**, Bhatia K, Coban S. Inflammation and Gastric Cancer. *Diseases* 2022; **10**: 35 [PMID: 35892729 DOI: 10.3390/diseases10030035]
16 **Cai J**, Zhong H, Wu J, Chen RF, Yang H, Al-Abed Y, Li Y, Li X, Jiang W, Montenegro MF, Yuan H, Billiar T, Chen AF. Cathepsin L promotes Vascular Intimal Hyperplasia after Arterial Injury. *Mol Med* 2017; **23**: 92-100 [PMID: 28332696 DOI: 10.2119/molmed.2016.00222]
17 **Bejarano L**, Jordão MJC, Joyce JA. Therapeutic Targeting of the Tumor Microenvironment. *Cancer Discov* 2021; **11**: 933-959 [PMID: 33811125 DOI: 10.1158/2159-8290.CD-20-1808]
18 **Mohamed MM**, Sloane BF. Cysteine cathepsins: multifunctional enzymes in cancer. *Nat Rev Cancer* 2006; **6**: 764-775 [PMID: 16990854 DOI: 10.1038/nrc1949]
19 **Krueger S**, Kalinski T, Wolf H, Kellner U, Roessner A. Interactions between human colon carcinoma cells, fibroblasts and monocytic cells in

coculture--regulation of cathepsin B expression and invasiveness. *Cancer Lett* 2005; **223**: 313-322 [PMID: 15896466 DOI: 10.1016/j.canlet.2004.09.050]

20 **Katunuma N**. Mechanisms and regulation of lysosomal proteolysis. *Revis Biol Celular* 1989; **20**: 35-61 [PMID: 2700097]

21 **Zheng X**, Chu F, Chou PM, Gallati C, Dier U, Mirkin BL, Mousa SA, Rebbaa A. Cathepsin L inhibition suppresses drug resistance in vitro and in vivo: a putative mechanism. *Am J Physiol Cell Physiol* 2009; **296**: C65-C74 [PMID: 18971393 DOI: 10.1152/ajpcell.00082.2008]

22 **Cuvier C**, Jang A, Hill RP. Exposure to hypoxia, glucose starvation and acidosis: effect on invasive capacity of murine tumor cells and correlation with cathepsin (L + B) secretion. *Clin Exp Metastasis* 1997; **15**: 19-25 [PMID: 9009102 DOI: 10.1023/a:1018428105463]

23 **Perez-Pacheco C**, Schmitd LB, Furgal A, Bellile EL, Liu M, Fattah A, Gonzalez-Maldonado L, Unsworth SP, Wong SY, Rozek LS, Rao A, Wolf GT, Taylor JMG, Casper K, Mierzwa M, D'Silva NJ. Increased Nerve Density Adversely Affects Outcome in Oral Cancer. *Clin Cancer Res* 2023; **29**: 2501-2512 [PMID: 37039710 DOI: 10.1158/1078-0432.CCR-22-3496]

24 **Garcia-Diaz C**, Pöysti A, Mereu E, Clements MP, Brooks LJ, Galvez-Cancino F, Castillo SP, Tang W, Beattie G, Courtot L, Ruiz S, Roncaroli F, Yuan Y, Marguerat S, Quezada SA, Heyn H, Parrinello S. Glioblastoma cell fate is differentially regulated by the microenvironments of the tumor bulk and infiltrative margin. *Cell Rep* 2023; **42**: 112472 [PMID: 37149862 DOI: 10.1016/j.celrep.2023.112472]

25 **Sudhan DR**, Siemann DW. Cathepsin L targeting in cancer treatment. *Pharmacol Ther* 2015; **155**: 105-116 [PMID: 26299995 DOI: 10.1016/j.pharmthera.2015.08.007]

26 **Condeelis J**, Pollard JW. Macrophages: obligate partners for tumor cell migration, invasion, and metastasis. *Cell* 2006; **124**: 263-266 [PMID: 16439202 DOI: 10.1016/j.cell.2006.01.007]

27 **Goswami S**, Sahai E, Wyckoff JB, Cammer M, Cox D, Pixley FJ, Stanley ER, Segall JE, Condeelis JS. Macrophages promote the invasion of breast carcinoma cells *via* a colony-stimulating factor-1/epidermal growth factor paracrine loop. *Cancer Res* 2005; **65**: 5278-5283 [PMID: 15958574 DOI: 10.1158/0008-5472.CAN-04-1853]

28 **Zhou BP**, Deng J, Xia W, Xu J, Li YM, Gunduz M, Hung MC. Dual regulation of Snail by GSK-3beta-mediated phosphorylation in control of epithelial-mesenchymal transition. *Nat Cell Biol* 2004; **6**: 931-940 [PMID: 15448698 DOI: 10.1038/ncb1173]

29 **Hansford S**, Kaurah P, Li-Chang H, Woo M, Senz J, Pinheiro H, Schrader KA, Schaeffer DF, Shumansky K, Zogopoulos G, Santos TA, Claro I, Carvalho J, Nielsen C, Padilla S, Lum A, Talhouk A, Baker-Lange K, Richardson S, Lewis I, Lindor NM, Pennell E, MacMillan A, Fernandez B, Keller G, Lynch H, Shah SP, Guilford P, Gallinger S, Corso G, Roviello F, Caldas C, Oliveira C, Pharoah PD, Huntsman DG. Hereditary Diffuse Gastric Cancer Syndrome: CDH1 Mutations and Beyond. *JAMA Oncol* 2015; **1**: 23-32 [PMID: 26182300 DOI: 10.1001/jamaoncol.2014.168]

30 **Kaszak I**, Witkowska-Piłaszewicz O, Niewiadomska Z, Dworecka-Kaszak B, Ngosa Toka F, Jurka P. Role of Cadherins in Cancer-A Review. *Int J Mol Sci* 2020; **21**: 7624 [PMID: 33076339 DOI: 10.3390/ijms21207624]

31 **Casanova-Acebes M**, Dalla E, Leader AM, LeBerichel J, Nikolic J, Morales BM, Brown M, Chang C, Troncoso L, Chen ST, Sastre-Perona A, Park MD, Tabachnikova A, Dhainaut M, Hamon P, Maier B, Sawai CM, Agulló-Pascual E, Schober M, Brown BD, Reizis B, Marron T, Kenigsberg E, Moussion C, Benaroch P, Aguirre-Ghiso JA, Merad M. Tissue-resident macrophages provide a pro-tumorigenic niche to early NSCLC cells. *Nature* 2021; **595**: 578-584 [PMID: 34135508 DOI: 10.1038/s41586-021-03651-8]

32 **Movahedi K**, Laoui D, Gysemans C, Baeten M, Stangé G, Van den Bossche J, Mack M, Pipeleers D, In't Veld P, De Baetselier P, Van Ginderachter JA. Different tumor microenvironments contain functionally distinct subsets of macrophages derived from Ly6C(high) monocytes. *Cancer Res* 2010; **70**: 5728-5739 [PMID: 20570887 DOI: 10.1158/0008-5472.CAN-09-4672]

33 **Qian BZ**, Pollard JW. Macrophage diversity enhances tumor progression and metastasis. *Cell* 2010; **141**: 39-51 [PMID: 20371344 DOI: 10.1016/j.cell.2010.03.014]

34 **Sica A**, Mantovani A. Macrophage plasticity and polarization: in vivo veritas. *J Clin Invest* 2012; **122**: 787-795 [PMID: 22378047 DOI: 10.1172/JCI59643]

35 **Kawai T**, Akira S. The role of pattern-recognition receptors in innate immunity: update on Toll-like receptors. *Nat Immunol* 2010; **11**: 373-384 [PMID: 20404851 DOI: 10.1038/ni.1863]

36 **Ngambenjawong C**, Gustafson HH, Pun SH. Progress in tumor-associated macrophage (TAM)-targeted therapeutics. *Adv Drug Deliv Rev* 2017; **114**: 206-221 [PMID: 28449873 DOI: 10.1016/j.addr.2017.04.010]

37 **Tian L**, Yu Q, Liu D, Chen Z, Zhang Y, Lu J, Ma X, Huang F, Han J, Wei L, Zhang L, Gao J, Wang L, Fu R. Epithelial-mesenchymal Transition of Peritoneal Mesothelial Cells Is Enhanced by M2c Macrophage Polarization. *Immunol Invest* 2022; **51**: 301-315 [PMID: 34490837 DOI: 10.1080/08820139.2020.1828911]

38 **Yu CC**, Chien CT, Chang TC. M2 macrophage polarization modulates epithelial-mesenchymal transition in cisplatin-induced tubulointerstitial fibrosis. *Biomedicine (Taipei)* 2016; **6**: 5 [PMID: 26872813 DOI: 10.7603/s40681-016-0005-5]

39 **He S**, Chen D, Hu M, Zhang L, Liu C, Traini D, Grau GE, Zeng Z, Lu J, Zhou G, Xie L, Sun S. Bronchial epithelial cell extracellular vesicles ameliorate epithelial-mesenchymal transition in COPD pathogenesis by alleviating M2 macrophage polarization. *Nanomedicine* 2019; **18**: 259-271 [PMID: 30981817 DOI: 10.1016/j.nano.2019.03.010]

40 **Hu Y**, Yuan M, Cheng L, Xu L, Wang G. Extracellular vesicle-encapsulated miR-25-3p promotes epithelial-mesenchymal transition and migration of endometrial epithelial cells by inducing macrophage polarization. *Mol Hum Reprod* 2024; **30**: gaae010 [PMID: 38407339 DOI: 10.1093/molehr/gaae010]

41 **Li L**, Sun P, Zhang C, Li Z, Cui K, Zhou W. MiR-98 modulates macrophage polarization and suppresses the effects of tumor-associated macrophages on promoting invasion and epithelial-mesenchymal transition of hepatocellular carcinoma. *Cancer Cell Int* 2018; **18**: 95 [PMID: 29989015 DOI: 10.1186/s12935-018-0590-3]

42 **Zhou X**, Chen H, Hu Y, Ma X, Li J, Shi Y, Tao M, Wang Y, Zhong Q, Yan D, Zhuang S, Liu N. Enhancer of zeste homolog 2 promotes renal fibrosis after acute kidney injury by inducing epithelial-mesenchymal transition and activation of M2 macrophage polarization. *Cell Death Dis* 2023; **14**: 253 [PMID: 37029114 DOI: 10.1038/s41419-023-05782-4]

43 **Zhou X**, Chen H, Shi Y, Li J, Ma X, Du L, Hu Y, Tao M, Zhong Q, Yan D, Zhuang S, Liu N. Histone deacetylase 8 inhibition prevents the progression of peritoneal fibrosis by counteracting the epithelial-mesenchymal transition and blockade of M2 macrophage polarization. *Front Immunol* 2023; **14**: 1137332 [PMID: 36911746 DOI: 10.3389/fimmu.2023.1137332]

44 **Hu Y**, Zhou C, Zhong Q, Li X, Li J, Shi Y, Ma X, Jiang D, Wang Y, Zhuang S, Liu N. LCZ696, an angiotensin receptor-neprilysin inhibitor, ameliorates epithelial-mesenchymal transition of peritoneal mesothelial cells and M2 macrophage polarization. *Ren Fail* 2024; **46**: 2392849 [PMID: 39165231 DOI: 10.1080/0886022X.2024.2392849]

45 **Murray PJ**, Allen JE, Biswas SK, Fisher EA, Gilroy DW, Goerdt S, Gordon S, Hamilton JA, Ivashkiv LB, Lawrence T, Locati M, Mantovani A, Martinez FO, Mege JL, Mosser DM, Natoli G, Saeij JP, Schultze JL, Shirey KA, Sica A, Suttles J, Udalova I, van Ginderachter JA, Vogel

SN, Wynn TA. Macrophage activation and polarization: nomenclature and experimental guidelines. *Immunity* 2014; **41**: 14-20 [PMID: 25035950 DOI: 10.1016/j.immuni.2014.06.008]

46 **Sindayigaya R**, Dogan C, Demtröder CR, Fischer B, Karam E, Buggisch JR, Tempfer CB, Lecomte T, Ouaissi M, Giger-Pabst U. Clinical Outcome for Patients Managed with Low-Dose Cisplatin and Doxorubicin Delivered as Pressurized Intraperitoneal Aerosol Chemotherapy for Unresectable Peritoneal Metastases of Gastric Cancer. *Ann Surg Oncol* 2022; **29**: 112-123 [PMID: 34611790 DOI: 10.1245/s10434-021-10860-y]

47 **Alyami M**, Hübner M, Grass F, Bakrin N, Villeneuve L, Laplace N, Passot G, Glehen O, Kepenekian V. Pressurised intraperitoneal aerosol chemotherapy: rationale, evidence, and potential indications. *Lancet Oncol* 2019; **20**: e368-e377 [PMID: 31267971 DOI: 10.1016/S1470-2045(19)30318-3]

48 **Chia DKA**, So JBY. Recent Advances in Intra-peritoneal Chemotherapy for Gastric Cancer. *J Gastric Cancer* 2020; **20**: 115-126 [PMID: 32595996 DOI: 10.5230/jgc.2020.20.e15]

49 **Gerber SA**, Rybalko VY, Bigelow CE, Lugade AA, Foster TH, Frelinger JG, Lord EM. Preferential attachment of peritoneal tumor metastases to omental immune aggregates and possible role of a unique vascular microenvironment in metastatic survival and growth. *Am J Pathol* 2006; **169**: 1739-1752 [PMID: 17071597 DOI: 10.2353/ajpath.2006.051222]

50 **Meza-Perez S**, Randall TD. Immunological Functions of the Omentum. *Trends Immunol* 2017; **38**: 526-536 [PMID: 28579319 DOI: 10.1016/j.it.2017.03.002]

51 **Mebius RE**. Lymphoid organs for peritoneal cavity immune response: milky spots. *Immunity* 2009; **30**: 670-672 [PMID: 19464991 DOI: 10.1016/j.immuni.2009.04.005]

52 **Coussens LM**, Werb Z. Inflammation and cancer. *Nature* 2002; **420**: 860-867 [PMID: 12490959 DOI: 10.1038/nature01322]

53 **Pollard JW**. Tumour-educated macrophages promote tumour progression and metastasis. *Nat Rev Cancer* 2004; **4**: 71-78 [PMID: 14708027 DOI: 10.1038/nrc1256]

54 **Sakamoto S**, Kagawa S, Kuwada K, Ito A, Kajioka H, Kakiuchi Y, Watanabe M, Kagawa T, Yoshida R, Kikuchi S, Kuroda S, Tazawa H, Fujiwara T. Intraperitoneal cancer-immune microenvironment promotes peritoneal dissemination of gastric cancer. *Oncoimmunology* 2019; **8**: e1671760 [PMID: 31741772 DOI: 10.1080/2162402X.2019.1671760]

55 **Gocheva V**, Wang HW, Gadea BB, Shree T, Hunter KE, Garfall AL, Berman T, Joyce JA. IL-4 induces cathepsin protease activity in tumor-associated macrophages to promote cancer growth and invasion. *Genes Dev* 2010; **24**: 241-255 [PMID: 20080943 DOI: 10.1101/gad.1874010]

56 **Shree T**, Olson OC, Elie BT, Kester JC, Garfall AL, Simpson K, Bell-McGuinn KM, Zabor EC, Brogi E, Joyce JA. Macrophages and cathepsin proteases blunt chemotherapeutic response in breast cancer. *Genes Dev* 2011; **25**: 2465-2479 [PMID: 22156207 DOI: 10.1101/gad.180331.111]

57 **Cristescu R**, Lee J, Nebozhyn M, Kim KM, Ting JC, Wong SS, Liu J, Yue YG, Wang J, Yu K, Ye XS, Do IG, Liu S, Gong L, Fu J, Jin JG, Choi MG, Sohn TS, Lee JH, Bae JM, Kim ST, Park SH, Sohn I, Jung SH, Tan P, Chen R, Hardwick J, Kang WK, Ayers M, Hongyue D, Reinhard C, Loboda A, Kim S, Aggarwal A. Molecular analysis of gastric cancer identifies subtypes associated with distinct clinical outcomes. *Nat Med* 2015; **21**: 449-456 [PMID: 25894828 DOI: 10.1038/nm.3850]

58 **Yonemura Y**, Nojima N, Kaji M, Fujimura T, Itoh H, Ninomiya I, Miyazaki I, Endo Y, Sasaki T. E-cadherin and urokinase-type plasminogen activator tissue status in gastric carcinoma. *Cancer* 1995; **76**: 941-953 [PMID: 8625219 DOI: 10.1002/1097-0142(19950915)76:6<941::aid-cncr2820760606>3.0.co;2-i]

59 **Locati M**, Curtale G, Mantovani A. Diversity, Mechanisms, and Significance of Macrophage Plasticity. *Annu Rev Pathol* 2020; **15**: 123-147 [PMID: 31530089 DOI: 10.1146/annurev-pathmechdis-012418-012718]

60 **Gwee YX**, Chia DKA, So J, Ceelen W, Yong WP, Tan P, Ong CJ, Sundar R. Integration of Genomic Biology Into Therapeutic Strategies of Gastric Cancer Peritoneal Metastasis. *J Clin Oncol* 2022; **40**: 2830 [PMID: 35649219 DOI: 10.1200/JCO.21.02745]

61 **Zheng X**, Chou PM, Mirkin BL, Rebbaa A. Senescence-initiated reversal of drug resistance: specific role of cathepsin L. *Cancer Res* 2004; **64**: 1773-1780 [PMID: 14996739 DOI: 10.1158/0008-5472.can-03-0820]

62 **Park JY**, Park KM. Recent discovery of natural substances with cathepsin L-inhibitory activity for cancer metastasis suppression. *Eur J Med Chem* 2024; **277**: 116754 [PMID: 39128327 DOI: 10.1016/j.ejmech.2024.116754]

63 **Li Y**, Ai X, Zou C, Liu Y, Ma L, Men J, Liu D, Sheng L, Ruan X, Liu H, Li W, Ma E, Yuan L. Discovery of a novel and selective cathepsin L inhibitor with anti-metastatic ability in vitro and in vivo against breast cancer cells. *Bioorg Chem* 2021; **115**: 105256 [PMID: 34426153 DOI: 10.1016/j.bioorg.2021.105256]

64 **Sudhan DR**, Rabaglino MB, Wood CE, Siemann DW. Cathepsin L in tumor angiogenesis and its therapeutic intervention by the small molecule inhibitor KGP94. *Clin Exp Metastasis* 2016; **33**: 461-473 [PMID: 27055649 DOI: 10.1007/s10585-016-9790-1]

65 **Sudhan DR**, Siemann DW. Cathepsin L inhibition by the small molecule KGP94 suppresses tumor microenvironment enhanced metastasis associated cell functions of prostate and breast cancer cells. *Clin Exp Metastasis* 2013; **30**: 891-902 [PMID: 23748470 DOI: 10.1007/s10585-013-9590-9]

66 **Almalki AA**, Shafie A, Hazazi A, Banjer HJ, Bakhuraysah MM, Almaghrabi SA, Alsaiari AA, Alsaeedi FA, Ashour AA, Alharthi A, Alharthi NS, Anjum F. Targeting Cathepsin L in Cancer Management: Leveraging Machine Learning, Structure-Based Virtual Screening, and Molecular Dynamics Studies. *Int J Mol Sci* 2023; **24**: 17208 [PMID: 38139037 DOI: 10.3390/ijms242417208]

67 **Li Q**, Wang H, Yang WL, Yang JK. An approach combining deep learning and molecule docking for drug discovery of cathepsin L. *Expert Opin Drug Discov* 2023; **18**: 347-356 [PMID: 36852432 DOI: 10.1080/17460441.2023.2174522]

Published by **Baishideng Publishing Group Inc**
7041 Koll Center Parkway, Suite 160, Pleasanton, CA 94566, USA
Telephone: +1-925-3991568
E-mail: office@baishideng.com
Help Desk: https://www.f6publishing.com/helpdesk
https://www.wjgnet.com